INSTITUTO SUPERIOR DE ENGENHARIA DO PORTO
MESTRADO EM ENGENHARIA QUÍMICA




REMOÇÃO DE FLUOXETINA POR BIOSSORÇÃO USANDO A MICROALGA CHLORELLA VULGARIS

DIANA ALEXANDRA FERREIRA FERNANDES
Outubro de 2019

POLITÉCNICO
DO PORTO

INSTITUTO SUPERIOR DE ENGENHARIA DO PORTO

MESTRADO EM ENGENHARIA QUÍMICA

REMOVAL OF FLUOXETINE BY BIOSORPTION USING THE MICROALGAE *CHLORELLA VULGARIS*

DIANA ALEXANDRA FERREIRA FERNANDES

2019

POLITÉCNICO
DO PORTO

REMOVAL OF FLUOXETINE BY BIOSORPTION USING THE MICROALGAE *CHLORELLA VULGARIS*

MASTER'S DEGREE IN CHEMICAL ENGINEERING - ENERGY AND BIOREFINERY

INSTITUTO SUPERIOR DE ENGENHARIA DO PORTO

Diana Alexandra Ferreira Fernandes

1140207

Supervisores:

Sónia Figueiredo

Olga Freitas

Paula Paíga

Acknowledgements

First of all, I would like to thank my supervisors and advisers at ISEP, Dr Sónia Figueiredo, Dr Olga Freitas and Dr Paula Paíga, for their direction, instructions, suggestions, kindness and inspiration during the project. I would also like to give a special thanks to Dr Andreia Silva for her availability and help through this process. All the information was very important to have a better and easy understanding of the work.

Finally, I would like to thank the opportunity to work with all the team and researchers from GRAQ - Grupo de Reação e Análises Químicas - research group of the Chemical Engineering Department from ISEP, which is integrated into the “Laboratório Associado para a Química Verde” (LAQV) of REQUIMTE.

This work was supported by UID/QUI/50006/2019 with funding from FCT/MCTES through national funds. The authors would like to thank also the EU and FCT/UEFISCDI/FORMAS for funding, in the frame of the collaborative international consortium REWATER financed under the ERA-NET Cofund WaterWorks2015 Call. This ERA-NET is an integral part of the 2016 Joint Activities developed by the Water Challenges for a Changing World Joint Programme Initiative (Water JPI).

Last but not less important, I would like to thank my parents and brothers, my friends that this institution gave me, for all their support throughout these two years as a master student at ISEP and during the work of this master thesis.

Abstract

Pharmaceuticals end up into the influent of municipal wastewater treatment plants (WWTPs). through the sewage system and due to the inability of conventional treatments to remove them, they are found on the environment. This work is focused on the contribution to the development of sustainable and economical tertiary treatments to remove pharmaceuticals in WWTPs.This study was developed within the scope of the international collaborative project REWATER, developed under the "Water Challenges for a Changing World Joint Program Initiative" (Water JPI).

The microalga *Chlorella vulgaris*, live and dead, was used as biosorbent to remove a pharmaceutical that is consumed worldwide, fluoxetine, from aqueous solutions.

Infrared spectroscopy characterization was made to living and lyophilized microalgae with and without being in contact with fluoxetine. This characterization allowed to identify the main functional groups, such as hydroxyl, sulfonic and carboxylic, that are probably involved in the biosorption process. The pH at the point of zero charge was 7.0 and 5.8 for living and dead microalgae, respectively. The study of the pH influence was performed. In relation to living microalgae, pH dependency was observed. As the initial pH increased, uptake adsorption of microalgae decreased. The reduction on the capacity was related to the pKa. The most favourable conditions for biosorption occur in pH range between 7.0 and 9.8 due to the electrostatic attraction between the positively charged fluoxetine and the negative charge alga surface. The effect of pH using lyophilized microalgae was inconclusive due to experimental problems.

Adsorption of fluoxetine by microalgae was described by a pseudo-second order kinetics at room temperature (20-24°C). Lyophilized microalgae showed a higher kinetic constant, being the ones that achieved equilibrium first (15 min) and removed 55% of the initial fluoxetine. The kinetic constants were $3.4\times10^{-4}\pm1.3\times10^{-4}$ and $5.4\times10^{-4}\pm1.3\times10^{-4}$ $g_{ALGAE}/(\mu g_{FLX}\cdot min)$, respectively for live and lyophilized microalgae. The equilibrium was reached by living microalgae within 20 min, for which 26% of fluoxetine was removed.

Equilibrium studies revealed that this system followed the Langmuir model (at 20-24°C). A higher adsorption capacity was observed for living microalgae, suggesting that other mechanisms (e.g. metabolic processes) besides adsorption may contribute to fluoxetine removal. The maximum capacities were $1.9\times10^{3}\pm0.1\times10^{3}$ and $1.6\times10^{3}\pm0.2\times10^{3}$ $\mu g_{FLX}/g_{ALGAE}$ for living and dead microalgae, respectively.

Although the microalga *Chlorella vulgaris* shows lower adsorption capacities than other adsorbents present in literature, its application is still promising due to their low cost, sustainability and in the case of lyophilized alga it is not affected by the presence of toxicants.

Keywords: biosorption, *Chlorella vulgaris*, fluoxetine, microalgae, pharmaceutical

Resumo

Os produtos farmacêuticos entram nas estações de tratamento de águas residuais (ETARs) através do sistema de esgotos e devido à incapacidade dos tratamentos convencionais de removê-los, estes entram no meio ambiente. Este trabalho pretende contribuir para o desenvolvimento de tratamentos terciários sustentáveis e económicos para remover fármacos em ETARs. Este estudo foi desenvolvido no âmbito do projeto colaborativo internacional REWATER, desenvolvido no âmbito da "Iniciativa Conjunta dos Desafios da Água para um Mundo em Mudança" (Water JPI).

A microalga *Chlorella vulgaris*, viva e liofilizada, foi utilizada como biosorvente para remover um fármaco que é consumido mundialmente, fluoxetina, de soluções aquosas.

A caracterização de espectroscopia infravermelho foi feita para microalgas vivas e liofilizadas com e sem contacto com fluoxetina. Essa caracterização permitiu identificar os principais grupos funcionais – como hidroxilo, sulfónico e carboxílico, que estão provavelmente envolvidos no processo de biossorção. O pH do ponto de carga zero foi de 7.0 e 5.8 para microalgas vivas e liofilizadas, respetivamente. O estudo da influência do pH também foi executado. Em relação às microalgas vivas, foi observada dependência do pH. À medida que o pH inicial aumentou, a biossorção pelas microalgas diminuiu. A redução na capacidade estava relacionada com o pKa. As condições mais favoráveis para a biossorção ocorreu numa gama de pH de 7.0 e 9.8 devido à atração electroestática entre a fluoxetina, carregada positivamente e a superfície da alga, carregada negativamente. O efeito do pH usando microalgas liofilizadas foi inconclusivo devido a problemas experimentais. Sugere-se repetir o estudo da influência do pH para tirar conclusões.

A adsorção de fluoxetina pela microalga foi descrita pelo modelo cinético de pseudo-segunda ordem, à temperatura ambiente (20-24ºC). As microalgas liofilizadas apresentaram uma constante cinética mais elevada, sendo as primeiras a atingir o equilíbrio (15 min) e removeram 55% da fluoxetina inicial. As constantes cinéticas foram $3.4\times10^{-4}\pm1.3\times10^{-4}$ e $5.4\times10^{-4}\pm1.3\times10^{-4}$ $g_{ALGAE}/(\mu g_{FLX}\cdot min)$, para a microalga viva e liofilizada, respetivamente. O equilíbrio foi atingido para as microalgas vivas em 20 min com uma remoção de fluoxetina de 26%.

Os estudos de equilíbrio revelaram que ambos os sistemas seguem o modelo de Langmuir (a 20-24ºC). Uma elevada capacidade de adsorção foi observada na alga viva, sugerindo que outros mecanismos (p.e. processos metabólicos), para além da adsorção, contribuíram para a remoção da fluoxetina. As capacidades máximas foram $1.9\times10^{3}\pm0.1\times10^{3}$ e $1.6\times10^{3}\pm0.2\times10^{3}$ $\mu g_{FLX}/g_{ALGAE}$ pelas microalgas vivas e mortas, respetivamente, à temperatura ambiente

Embora a microalga *Chlorella vulgaris* mostre menor capacidade de adsorção do que outros adsorventes presentes na literatura, a sua aplicação é promissora devido ao seu baixo custo, sustentabilidade e, no caso de algas liofilizadas, não é afetada pela presença de substâncias tóxicas.

Palavras-passe: biossorção, *Chlorella vulgaris*, fármaco, fluoxetina, microalga

Contents

List of figures

Abbreviations

AIC	Akaike information criterion
APIs	Active pharmaceutical ingredients
BIC	Bayesian information criterion
BOD_5	Biochemical oxygen demand
COD	Chemical oxygen demand
E2	17-beta-estradiol pharmaceutical
EE2	17-alpha-ethinylestradiol pharmaceutical
ERA	Environment risk assessments
EU	European Union
FLD	Fluorescence detector
GRAQ	Grupo de Reação e Análises Químicas
HPLC-FLD	High Performance Liquid Chromatography with fluorescence detector
LAQV	"Laboratório Associado para a Química Verde"
MBBR	Moving bed biofilm reactor
MBR	Membrane bioreactor
PACs	Pharmaceutical active compounds
PZC	Point of zero charge
REACH	Authorisation and Restriction of Chemicals
ROS	Reactive oxygen species
WFD	Water Framework Directive
WWTPs	Wastewater treatment plants

Nomenclature

a_{RP}	Redlich-Peterson model parameter
C_{ALGAE}	Biomass (algae) concentration
C_{FLX}	Concentration of the fluoxetine at time t
$C_{FLX,EQ}$	Equilibrium biosorbate concentration
$C_{FLX,0}$	Initial concentration of the adsorbate concentration
C_{ID}	Thickness of the boundary layer
d.f.	Degree of freedom
$d.f._{REF}$	Degree of freedom of reference model
F_{calc}	Coefficient of variances of two different models
$FI_{485/645}$	Fluorescence intensity that transmits 485/20 nm light and an emission filter that transmits 645/40 nm light
$F_{\alpha,d.f._1,d.f._2}$	Tabulated value of the Fisher distribution, called critical F,
K_1	Equilibrium rate constant of pseudo-first order adsorption
K_2	Equilibrium rate constant of pseudo-second order adsorption
K_{EXT}	External mass transfer constant
K_F	Freundlich isotherm constant
K_{FH}	Flory-Huggins equilibrium constant
K_{ID}	Intraparticle diffusion rate constant
K_L	Langmuir adsorption constant
K_{RP}	Redlich-Peterson model parameter
K_s	Sips isotherm constant
K_T	Tóth isotherm constant
m_{ALGAE}	Mass of adsorbent
MS	Sips model exponent
N	Number of experimental data
n_F	Freundlich exponent
n_{FH}	Exponent of the Flory-Huggins model
n_T	Tóth isotherm constant
P	Number of constants in the model
pH_{FINAL}	Final pH
$pH_{INITIAL}$	Initial pH
pH_{PZC}	Point of zero charge pH
Ka	Acidity constant
q_{CAL}	Capacity of adsorption of adsorbent calculated from one of the models
$q_{CAL,EQ}$	Amount of adsorbate sorbed at equilibrium by the model
q_{EXP}	Experimental determined capacity of adsorption of adsorbent
$q_{EXP,AVG}$	Mean of the experimental determined capacity of adsorption of adsorbent
$q_{MAX,L}$	Maximum uptake capacity of the adsorbents of Langmuir model

$q_{MAX,T}$	Maximum uptake capacity of the adsorbents of Tóth model
q_{MS}	Sips maximum adsorption capacity
R^2	Coefficient of determination
R^2_{adj}	Adjusted coefficient of determination
R_L	Dimensionless separation factor
S_{EXT}	Specific surface area
SSE	Sum of the square of the errors
SSE_{REF}	Sum of the square of the errors of reference model
$S_{y.x}$	Standard error of estimate
T	Time
V_{SOL}	Solution volume
X^2	Non-linear chi-squared test
X^2_{red}	Reduced non-linear chi-squared test
α_E	Initial adsorption rate constant of Elovich model
β_E	Constant of desorption related to the extent of surface coverage and to the Activation energy for chemisorption of Elovich model
β_{RP}	Exponential value of Redlich-Peterson model parameter
Θ	Degree of surface coverage

1. Introduction

Pollution has been affecting negatively the environment and, nowadays one of the most emerging issues is water pollution (Mishra et al., 2017).

The aquatic contaminants found in lakes, rivers and seas are originated by the discharge of domestic or industrial wastewaters with inadequate treatment or by agriculture run-off. Organic and inorganic aquatic pollutants, such as heavy metals, pharmaceuticals and pesticides, can directly affect both aquatic and human life, and along the food chain (Mishra et al., 2017). The standard of living, accessibility to medicines and average life expectancy have been increasing gradually over the years, so consequently, it is predictable that their consumption will increase (Kümmerer, 2004) and so their concentration in domestic wastewaters. The introduction of treatments that can reduce their concentration in order to reach the levels required by the regulation is needed (Mishra et al., 2017).

1.1 Pharmaceuticals

Pharmaceuticals contain several active pharmaceutical ingredients (APIs), excipients, additives, inorganic salts and organic chemicals such as sugars, pigments and dyes (Kümmerer, 2004). Pharmaceutical active compounds (PACs) are included in the emerging contaminants (Escapa et al., 2015) and can be categorized accordingly to their functionality, such as antibiotics, analgesic, antineoplastic, anti-inflammatory, or according to their chemical structure, being the latest used to classify the sub-groups of the active substances. PACs are considered complex substances with diverse functions, physicochemical and biological proprieties (Kümmerer, 2004) and may produce different environment exposure profiles (Pereira et al., 2015).

Some of the pharmaceuticals are typically polar or charged, and may be lipophilic or hydrophilic, which means that some will connect easily to the fatty tissues, to the sludge and suspended particles in water, while others tend to be dissolved (Borao, 2015).

1.2 Effects

Although the concentration of these substances, found in the environment, were low from ng/L to µg/L, they may cause negative impacts not only directly in the environment but also they may cause health risks, such as short and long-term toxicity (Borao, 2015).

For example, in some countries of Asia, it is forbidden to manufacture and use of diclofenac in veterinary because it may lead to the extinction of local vultures. Diclofenac, a non-steroidal anti-inflammatory medicine, is used to treat inflammation, pain and fever in domestic livestock, in particular in cows. In the case of cow deaths, vultures ingest diclofenac indirectly by consuming cow carcasses of livestock that had been treated with diclofenac before death. This medicine triggers an acute kidney failure which causes death in a few days. Currently, three species of vultures are endangered due to intoxication by this medicine (Kümmerer et al., 2010).

There are already studies that report the possibility of sex hormones, such as 17-beta-estradiol and 17-alpha-ethinylestradiol, being related with the disrupt of the endocrine system in

humans and inhibition of fish reproduction, even in low concentrations (Borao, 2015; Kümmerer et al., 2010).

The effects of pharmaceuticals have been studied individually, however, humans are exposed to a mixture of medicines which may cause other effects that are not properly studied yet (Doerr-MacEwen, 2007).

1.3 Occurrence

The most common ways to administrate these substances are orally or intravenously and this is a factor that can influence their metabolism. Some substances can be metabolized before being excreted, while others are moderately or practically unmetabolized or not metabolized. Consequently, APIs can be detected in municipal sewage together with their metabolites and if they are not efficiently treated, numerous pharmaceuticals end up in the aquatic ecosystems and may be a possible source of contamination of water directed to the human consumption (Kümmerer, 2004).

In addition, unused and outdated pharmaceuticals flushed down in household drains are another way to pharmaceuticals entering in the environment.

Households, institutions such as hospitals, agriculture, livestock and industries are also known as sources of pharmaceuticals that come into the environment (Figure 1.1) (Wilt, 2018).

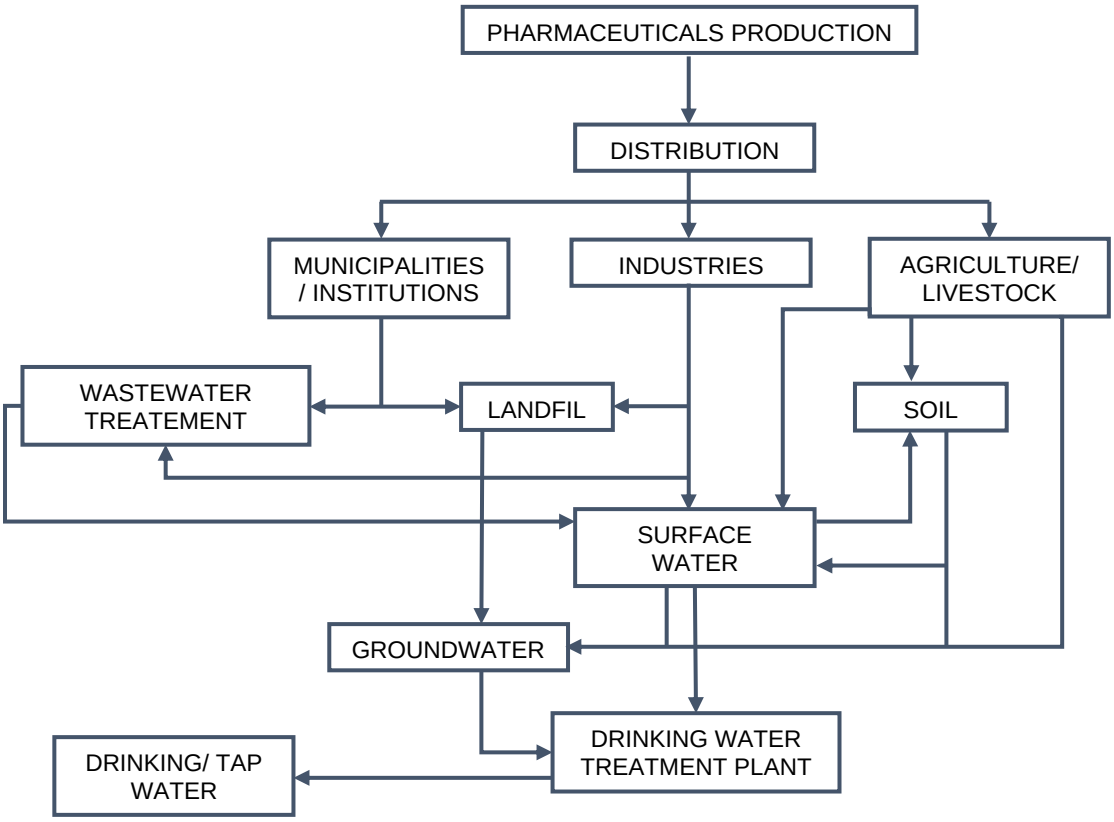

Figure 1.1. Pathways of input and distribution of pharmaceuticals and other micropollutants in the environment from production to drinking water (Adapted from Barbosa et al., 2016).

The concern of contamination by PACs has risen in the last two decades because its consumption, particularly in developed countries, has been increasing and due to development of technology and sophistication of advanced analytical methodologies that can reach very low detection levels of PACs in water (Doerr-MacEwen, 2007). PACs were detected not only in medical care units effluents, raw and treated sewage, and landfill sites but also on surface water, groundwater and it was already detected in low concentrations (up to 0.1 µg/L) in some drinking water sources (Kümmerer, 2004; Wilt, 2018).

The consumption of pharmaceuticals varies from country to country. In the European Union (EU), about 3000 medical substances are used and worldwide consumption has been increasing (Wilt, 2018). Portugal is not an exception and between 2013 and 2018, the number of pharmaceutical packages increased 7.4%, from 14.9 to 16.1 millions of packages (Figure 1.2) (INFARMED, 2017, 2018).

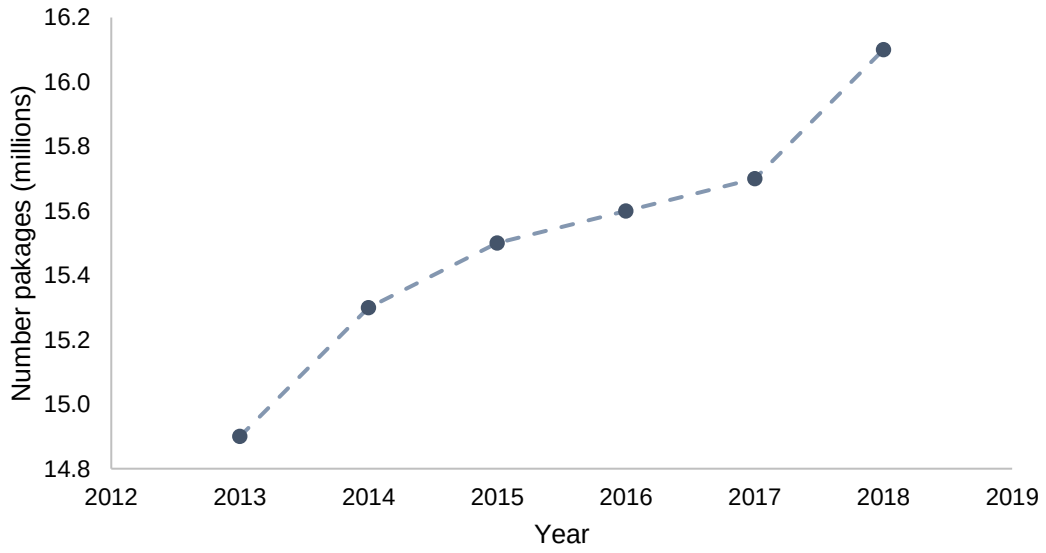

Figure 1.2. Consumption of pharmaceuticals by the number of packages in millions for each year, between 2013 and 2018 in Portugal national health system (Adapted from INFARMED, 2018, 2017).

In Portugal, the most consumed pharmaceuticals are alprazolam, lorazepam and zolpidem (anxiolytics and hypnotics), azithromycin and ciprofloxacin (antibiotics), simvastatin, bezafibrate and gemfibrozil (lipid regulators), ibuprofen, diclofenac and paracetamol (non-steroidal anti-inflammatories and analgesics agents) (Pereira et al., 2014).

In the Portuguese pharmaceuticals consumption balance for 2018, the active substances with the most use were atorvastatin and simvastatin (antilipermics/ lipid regulators), paracetamol (analgesic and antipyretic), metformin (insulins and oral antidiabetics), amoxicillin and clavulanic acid (antibiotic), bisoprolol (anti-hypertensive), acetylsalicylic acid (anticoagulants and antithrombotic), alprazolam (anxiolytics) and pantoprazole and omeprazole (antacids and anti-ulcerous) (INFARMED, 2018).

Worldwide, antidepressants are considered one of the most consumed pharmaceuticals. In England, 2.83 tonnes of fluoxetine and 2.74 tonnes of sertraline had been consumed in 2000 and they are only two examples between dozens of them in the pharmaceutical market (Sebastine et al., 2003).

In Pereira et al. (2014) studies, the efficiency of pharmaceutical removal in the conventional treatment of wastewater in wastewater treatment plants (WWTPs) was evaluated. Conclusions were taken, such as the anti-inflammatory group was the most efficiently removed, being the biggest contributor to the good efficiency, paracetamol (around 99.9%). Unlike diclofenac, which has the lower removal efficiency (around 45.6%). Lipid regulators and antibiotics showed a high removal efficiency, 87.9% and 79.3%, respectively. On the other hand, anxiolytics such as alprazolam and lorazepam were not removed. According to Lajeunesse et al., (2012), neurotic compounds such as carbamazepine and venlafaxine had a mean removal rate around 12% and fluoxetine, close to 60%.

Persistence is an important feature to judge the behaviour of substances in the environment (Kümmerer et al., 2010) and it is related to the presence of a chemical in the environment that it is even detected far from the source through continuous monitoring. This definition cannot be applied directly to pharmaceuticals, since pharmaceuticals are discharged constantly to the aquatic environment through sewage treatment plants at a higher daily mass loads than environmental removal rates. For this reason, pharmaceuticals are classified as pseudo-persistent (Bu et al., 2016). The persistence of organic pollutants is proportional to the numerous long-term effects and the longer the exposure to these substances, the greater the possibility of various ecosystem contaminations (Kümmerer et al., 2010). Fluoxetine and carbamazepine are some of the neurotic compounds which showed to persist in the aqueous environment (Kwon et al., 2006).

1.4 Legislation

Since it is not possible to avoid the exposure of aquatic environment to the pharmaceuticals, the risk assessment of medicines is an important tool to ensure that the concentration of pharmaceuticals meets the Water Framework Directive (WFD) of the European Union (EU) (Pereira et al., 2015). Until now, regulations associated with the discharge of pharmaceuticals do not exist and consequently, there are no limit values or standards for them. The existence of this gap in legislation is due to the insufficient information and lack of consensus on the substances. However, sooner it would be necessary to create legislation to regulate this subject since long-term exposure of these will increase the risk of adverse effects on the aquatic ecosystem and human health (Borao, 2015).

The European Parliament has updated the Directives 2000/60/EC and 2008/105/EC, setting the aim of creating a monitoring list, a “watch list”, of the potentially harmful substances or group of substances in order to collect data and develop analytic methods (without associated excessive costs). The substances included in this list represent a risk to the aquatic environment of the European Union (European Parliament, 2013). The most recent directive is the Directive

2013/39/EU, however, it may change continuously since the list of pharmaceuticals is very dynamic and it may be adapted according to the persistence in the water life cycle, which results in its limited validity. For the first time, three pharmaceuticals were included in the "watch list" of priority substances: diclofenac (CAS 15307-79-6), 17-beta-estradiol (E2) (CAS 50-28-2) and 17-alpha-ethinylestradiol (EE2) (CAS 57-63-6) (European Parliament, 2013). According to this Directive, effluents need to be monitored with the purpose to keep the data updated and, in some cases, to prioritize. For that, Environmental Risk Assessment (ERA), which include ecotoxicological and toxicological effects studies, are being made in order to evaluate aquatic and human health impacts (Pereira et al., 2015).

Generally, the evaluation of the wastewater treatment efficiency is determined by the percentage removal, since there are no guidelines and standards with maximum values for the discharge of pharmaceuticals in the environment. Nevertheless, it may be more interesting and important to pay attention to the concentration of pharmaceuticals after treatments (Borao, 2015).

1.5 Goal and objective

This work intends to contribute to the development of sustainable and economical tertiary treatments to remove pharmaceuticals which posteriorly can be applied in municipal wastewater treatment plants. This study was developed within the scope of the international collaborative project REWATER, developed under the "Water Challenges for a Changing World Joint Program Initiative" (Water JPI) from February to July 2019 in the Grupo de Reação e Análises Químicas (GRAQ) research group. GRAQ is a multidisciplinary team of researchers that are focused on promoting innovation in analytical chemistry, environment and sustainability areas. This group is integrated into the "Laboratório Associado para a Química Verde" (LAQV) of REQUIMTE.

The aim of the present study is to investigate the removal of pharmaceuticals (e.g. fluoxetine) by biosorption using live and dead microalgae (e.g. *Chlorella vulgaris*). This work will include several steps: pharmaceutical selection; kinetic and equilibrium studies in aqueous solutions, in a closed system.

1.6 Structure

The report is divided into 7 main chapters: Introduction, Background Information, Tertiary Wastewater Treatment by Microalgae, Adsorption Process Models, Experimental Description, Results and Discussion and lastly, Conclusions and Future Suggestions.

The Introduction chapter gives a brief information about the current state of pharmaceutical use, explaining its presence in wastewater and the effects they may cause. In addition, it still mentions the current legislation applied to this field. Chapter 2, Background Information, will present information about the steps involved in conventional wastewater treatment, from preliminary to tertiary treatments. Then, the alternative tertiary treatment by microalgae will give an overview in Tertiary Wastewater Treatment by Microalgae (Chapter 3), microalgae properties and pharmaceutical removal mechanisms, such as biosorption, bioaccumulation and intracellular biodegradation, by these microorganisms as well. Kinetic and equilibrium models and error

analysis methods will be introduced in Chapter 4, Adsorption Process Models. Experimental descriptions will be focus in Chapter 5. The results are compared and discussed based on the available literature in Chapter 6. And finally, the work will be summarized in Chapter 7, where the main conclusions will be presented, and some possible future research directions will be suggested.

2. Wastewater treatment

2.1 Urban wastewater

All untreated effluent that comes from municipalities, industries, commercial activities and stormwater is labelled as wastewater. Its composition depends on its source and can be categorised according to it (Guldhe et al., 2017; Sonune et al., 2004). The pharmaceuticals present in wastewater come from urban and industrial effluents such as pharmaceutical and farming industries.

Urban wastewater is a blending of industrial, domestic influents and stormwater. Domestic wastewater corresponds to the water that is discharged from residences, commercial institutions and other facilities and is the largest share of the municipal wastewater. In industries subcategory, there are wastewater streams from several industries, such as steel, pharmaceutical, chemical, textile, food processing, paper pulp, sugar. Its composition consists of a high concentration of biodegradable and non-biodegradable organic matter, inorganic matter and potential inhibitory substances. On the other hand, it may show a low concentration of nutrients and high concentration of heavy metals and toxic compounds. Stormwater results from the rainfall drainage. Urban wastewater benefits from the presence of nutrients, such as ammonia and phosphate, provided by domestic wastewaters, which are usually absent in industrial wastewaters and storm waters. The main components of this type of wastewater are biodegradable organic matter, nutrients (nitrogen and phosphorous), which allows the application of biological treatments to urban wastewaters (Guldhe et al., 2017).

2.2 Conventional wastewater treatment

Domestic and industrial wastewaters present a high amount of organic and inorganic material, and pathogenic microorganisms, pharmaceuticals and toxic compounds. Unless the wastewater is not treated, these effluents will cause eutrophication and contamination of soil, surface water and groundwater. Thus, conventional wastewater treatment was designed to remove contaminants from the water with the purpose to achieve water with quality to be discharged or reused (Mishra et al., 2017), however, currently, it is not designed to remove pharmaceuticals (Wilt, 2018). Sewage systems bring wastewater from the different industrial sectors and municipalities that are treated in WWTPs (Borao, 2015). The conventional WWTPS (Figure 2.1) are classified as preliminary, primary, secondary and tertiary (Abdel-Raouf et al., 2012; Mishra et al., 2017) according to the level of treatment reached.

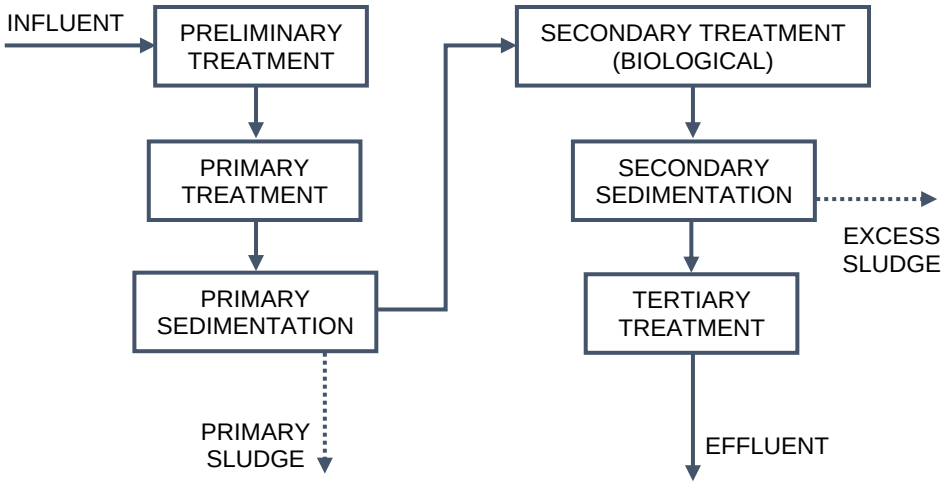

Figure 2.1. Conventional wastewater treatment (Adapted from Petrović et al., 2013).

Although, this treatment is the most common currently, it has some disadvantages such as lack of efficiency to biodegrade all type of contaminants, such as detergents, pesticides and heavy metals, which limit the use of sludge as soil fertilizer because it can lead to soil contamination and pollution of surface and groundwater resources (Borao, 2015; Kadhim, 2014). When chemical processes are used it is costly to operate and generate a large amount of sludge contaminated with chemicals (Mishra et al., 2017), leads to secondary pollution due to the chemicals used (Abdel-Raouf et al., 2012). Furthermore, environmental regulations are getting stricter which forces the adoption of advanced and sustainable methods (Cuellar-Bermudez et al., 2017).

2.2.1 Preliminary treatment

The goal of the preliminary treatment is to remove large, suspended and floatable material from the raw wastewater (Mishra et al., 2017) that could block the flow through the plant or even damage the equipment (Abdel-Raouf et al., 2012). The sewage goes through a bar screen and a grit chamber, so large and rough inorganic and organic solids may be filtered out and removed (Mishra et al., 2017).

2.2.2 Primary treatment

After the preliminary treatment, primary treatment is applied and allows the sedimentation of settleable solids, as primary sludge, in the bottom of the primary clarifier tank and removes grease and oils, in the surface. Generally, in this process, 50-65% of suspended solids and 30-40% of the organic biodegradable matter are removed (Mishra et al., 2017).

At this stage, there are studies that show that the removal efficiency of certain pharmaceuticals was low, for example, around 28% of diclofenac and estriol were removed, unlike ibuprofen and naproxen that were not removed after primary treatment. This may be explained by affinity proprieties of each pharmaceutical lipophilic compounds are more likely to be attached with grease and oil and hydrophilic compounds tend to be dissolved in water (Borao, 2015).

2.2.3 Secondary treatment

The aim of the secondary treatment is to remove biodegradable organic material by biological degradation. Biological processes such as activated sludge process, rotating bioreactor contactor, trickling filter, fluidized bed reactors may be used (Yildiz, 2012). The most used is the activated sludge process, in which aerobic microorganisms oxidize the organic material in the aeration tank. This step of the process requires air (oxygen) supply which involves extra costs. After that, the wastewater follows to the secondary clarifier where the biological sludge settles and is separated. Although secondary treatment achieves a 90 to 95% removal of organic biodegradable matter (Mishra et al., 2017), nitrogen and phosphorus present low removal efficiencies. Therefore a tertiary treatment may be needed to remove nutrients in order to avoid eutrophication of the aquatic environment (Abdel-Raouf et al., 2012).

Since the removal of pharmaceuticals in WWTPs is not a regulated parameter, WWTPs are not designed to remove them, however, several studies report that biological treatments are able to remove some of them (Wilt, 2018). There are studies in which 100% removal of substances such as ibuprofen and paracetamol were achieved. However, for some pharmaceuticals such as metropolol, the concentration at the effluent raised compared to the concentration at the influent, which can be explained by the presence of input conjugate compounds that are changed into the quantified compounds through treatment (Radjenovic et al., 2006; Wilt, 2018). Biodegradation is not considered efficient enough to remove pharmaceuticals for some reasons: the concentration of these substances in wastewater is lower compared to other pollutants which may not allow active enzymes to remove pharmaceuticals; the chemical structure of some pharmaceuticals is sufficiently stable; many pharmaceuticals have the ability to inhibit microorganisms growth and consequently it would not be possible to use them as energy or carbon source for metabolism of microorganisms (Borao, 2015; Wilt, 2018).

2.2.4 Tertiary treatment

Tertiary treatment is used to remove a group or a specific contaminant from the wastewater, such as nutrients (nitrogen, phosphorus), heavy metals, organic and inorganic micropollutants thin suspended particle and pathogenic microorganisms.

Tertiary treatment is also used to allow the reuse of treated wastewater in industry, agriculture and human uses (Mishra et al., 2017). Besides biological treatment, there are chemical treatment processes such as advanced oxidation processes, which may involve photolysis, photocatalysis and oxidation, using ozone or hydrogen peroxide or UV light/ Fenton (Fe^{2+}/ H_2O_2). Chemical oxidation methods are popular processes used to treat wastewater from the pharmaceutical industry (Escapa *et al.*, 2015). Despite good results obtained by the chemical processes, they involve extra chemicals, materials and energy which leads to high operational costs and can produce by-products that may be more harmful than the original compounds (Wilt, 2018). Physical processes, like membrane filtration or sorptive processes, using activated carbon, show promising results in the removal of pharmaceuticals.

3. Tertiary wastewater treatment by microalgae

The conventional wastewater treatments are not efficient enough to remove completely pharmaceuticals (Bodin et al., 2016). According to Bodin et al. (2016), through biotransformation is possible to remove 22–99% of pharmaceuticals in wastewater treatment plant along with sorption onto sewage sludge. Although there is not much knowledge about it, there are already some studies about pharmaceuticals biotransformation using microalgae (Escapa et al., 2015).

3.1 Microalgae properties

Most of the microalgae are eukaryotic photosynthetic organisms, except blue-green algae (*Cyanobacteria*), which are prokaryotic (Kadhim, 2014). Microalgae represent a large group of microorganisms which can be found in freshwater, brackish water, seawater and wastewater. Proteins, carbohydrates, lipids, fatty acids, pigments, vitamins and enzymes are some of the constituents of the microalgae cells. Light, carbon source, macronutrients (nitrogen and phosphorus), micronutrients and some metals (Xiong et al., 2018) are required for their growth.

Microalgae can be used for multiple purposes and lately they have established significant attention to their role in rehabilitation of environment and production of microalgal biomass than be used in different industries, such as feedstock for biofuels and biogas (Hom-Diaz et al., 2017; Kadhim, 2014), bioactive molecules, pigments (Escapa et al., 2015), nutraceuticals, animal feed and organic fertilizer (Kadhim, 2014). Another purpose that could be given to algae biomass is using it as fertilizer in agriculture however it would reintroduce the removed pollutants (e.g. pharmaceuticals) into the food chain (Wilt, 2018). However, one of the challenges of using microalgae in wastewater treatment is the separation of microalgae from the effluent after treatment due to the small size of microalgae, low density difference. Some factors such as the value of the target products/ species, the biomass concentration, the size of microalgae cells and the desired final product will influence on the separation technique choice. There are several techniques to harvest microalgae such as centrifugation, flocculation, filtration, gravity sedimentation, flotation and electrolytic methods. Flocculation associated with flotation/ sedimentation process followed by dewatering using centrifugation or sedimentation have shown to be good alternatives (Escapa et al., 2015). But due to the large amounts of wastewater treated and small value of biomass, the most common technique is sedimentation, however, it only fits for large microalgae (ca. >70 μm) (Hom-Diaz et al., 2017).

In the wastewater treatment, several microalgae species have been used depending on some aspects such as wastewater features and environmental circumstances. According to Kadhim (2014), *Chlorella* and *Scenedesmus* species are the most common microalgae strains in wastewater, being *Chlorella* species those who show to be more tolerant, adaptive and resistant to different physical and biochemical conditions (Kadhim, 2014). In Table 3.1, it is demonstrated that different microalgae species have the capacity to remove pharmaceutical contaminants from the wastewater (Xiong et al., 2018).

Table 3.1. Microalgal species used in bioremediation of wastewater and pharmaceuticals contaminants (Adapted from Xiong et al., 2018).

Phylum	Genus	Species	
Cyanobacteria	*Microcystis*	*aeruginosa*	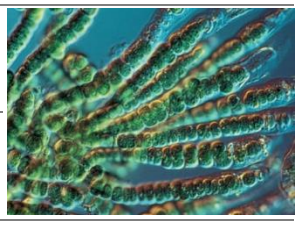
	Spirulina	*platensis*	
Bacillariophyta	*Chaetoceros*	*calcitrans*	
	Nitzschia	*closterium*	
	Halamphora	*coffeaeformis*	
	Thalassiosira	*pseudonana*	
Euglenophyta	*Euglena*	*agilis*	
		gracilis	
Chlorophyta	*Chlamydomonas*	*mexicana*	
		reinhardtii	
	Chlorella	*vulgaris*	
		pyrenoidosa	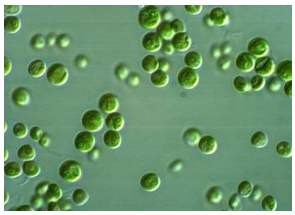
		sorokiniana	
		minussima	
		kessleri	
		protothecoide	
		zofingiensis	
	Nannochloris		
	Stigeoclonium		
	Klebsormidium		
	Micractinium		
	Raphidocelis	*subcapitata* [1]	

[1] *Raphidocelis subcapitata* was formerly known as Selenastrum capricornutum and Pseudokirchneriella subcapitata (Yamagishi et al., 2017).

Chlorophyta	*Scenedesmus*	*obliquus*	
		dimorphus	
		acutus	
		platensis	
		quadricauda	
	Ankistrodesmus		
	Cosmarium		
	Desmodesmus	*subspicatus*	
	Neochloris	*oleoabundans*	

3.2 Mechanisms of pharmaceutical removal by microalgal

The mechanisms that allow removing pharmaceuticals using microalgae include biosorption, bioaccumulation, and intracellular and extracellular biodegradation (Xiong et al., 2018).

3.2.1 Biosorption

The sorption differs according to the hydrophobicity, structure and functional groups of the pharmaceuticals and microalgae species. This mechanism is based on the charge of the cell surface of the microalgae. The cell wall has an overall negative charge due to the dominant functional groups, such as carboxyl, phosphoryl and amine, that allows to bind and attract cations. If the pharmaceuticals have cationic groups, these will be attracted to the surface of the microalgae due to the electrostatic interaction and this is called biosorption (Xiong et al., 2018). Different processes (Figure 3.1) are involved in biosorption such as biosorption, chelation/ complexation, ion exchange and surface precipitation (Bilal et al., 2018).

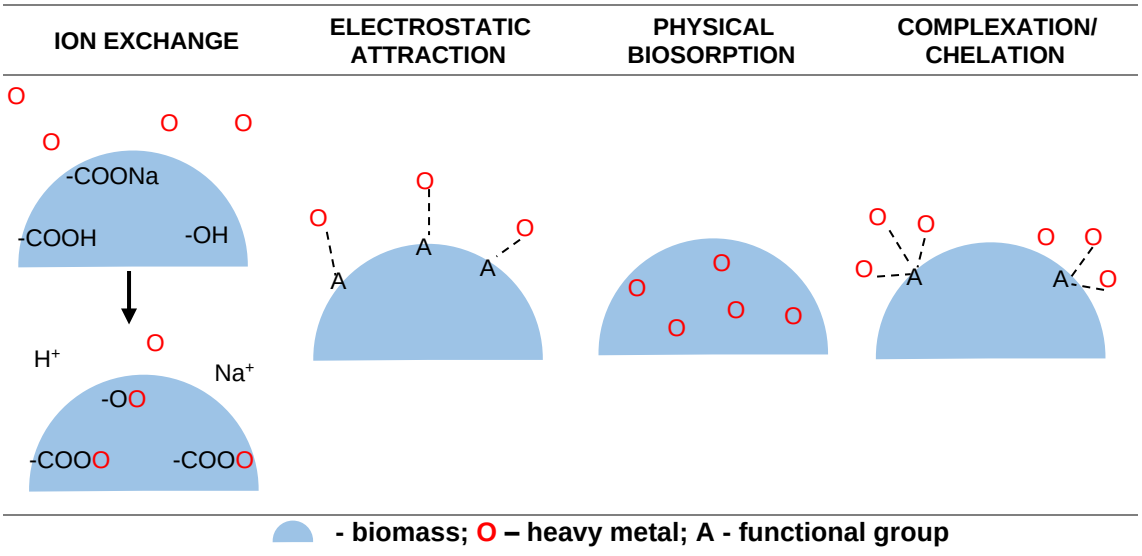

Figure 3.1. Representation of the mechanisms involved in the biosorption: ion exchange, electrostatic attraction, physical biosorption and complexation/ chelation (Adapted from Bilal et al., 2018).

Since biosorption is considered a metabolism independent, it may occur in both live and dead cells. According to Tam et al. (2002), dead microalgal species were more efficient in removing pollutants than live microalgae and they show some advantages as they are not affected by the pollutants, it is easier to handle them, do not require extra costs related to nutrients and it is possible to use them for many cycles.

Some factors that affect biosorption are pH, temperature, initial metallic concentration, contact time, competing ions and biosorbent dosage, being pH the most important factor. In relation to temperature, varying this parameter may change thermodynamic parameters and biosorption capacity. Increasing the contact time increases biosorption efficiency, however after all sites of the biosorbent achieve saturation, the biosorption remains stable since it was achieved an equilibrium state. High initial pollutant concentration (higher driving force for mass transfer) and high doses of biosorbent (more available free sites), increase the efficiency of the biosorption process (Bilal et al., 2018).

3.2.2 Bioaccumulation

Bioaccumulation is a slower stage comparison to the previous one (Tam et al., 2002). This stage of the process depends on the metabolism of a living organism that can remove compounds, driven by energy. When pharmaceuticals accumulate in microalgae cells and achieve a certain concentration of PACs, there is a generation of reactive oxygen species (ROS). ROS do not prejudice control cellular metabolism, on contrary, they are crucial for the control, however ROS in excess degrade cellular compounds and in some cases, they can genetically modify cells which can lead to the inhibition of the cell activity (Xiong et al., 2018).

3.2.3 Intracellular biodegradation

This stage is considered the most effective to eliminate organic compounds by microalgae (Xiong et al., 2018), however it depends strictly on the species because to different species, there are different origins, shapes, sizes, cell wall composition, uptake capacities and enzymes systems (Tam et al., 2002). Due to their catalytic ability, microalgae can degrade complex compounds. There are already studies that had shown that 30-80% of the pharmaceutical compounds from urban wastewater were biodegraded by these microorganisms (Xiong et al., 2018).

Microalgae have an enzyme system that is categorized into two groups: phase I and phase II. Firstly, in phase I, there is an increase of hydrophobicity of the compound due to the addition or exposure of a hydroxyl group. This step includes hydrolysis, oxidation or reduction reactions which end up biodegrading contaminants. After these reactions, the phase II enzyme group has the function to excrete contaminants from intracellular with the purpose to protect the cell against oxidation (Xiong et al., 2018).

3.2.4 Extracellular biodegradation

Microalgae can expel extracellular polymeric substances to their vicinity, and they will behave as a digestive system because they keep extracellular enzymes around to the cells giving

the possibility to metabolize heavy metals and organic compounds on the surface. Thus, this process allows the degradation of compounds, such as pharmaceuticals, and consequently the detoxification (Tam et al., 2002; Xiong et al., 2018).

3.3 Factors that influence biosorption

pH, temperature, initial metallic concentration, contact time, competing ions and biosorbent dosage are some factors that affect biosorption, which pH is the most important factor. Increasing pH will increase biosorption as well, however for high levels of pH, can produce undesirable precipitation and for low levels of pH, can reduce sorption capacity by the repulsion between protonated groups and the positive charge of the pharmaceuticals. In relation to temperature, varying this parameter may change thermodynamic parameters and biosorption capacity. Increasing the contact time increases biosorption however after all sites of the biosorbent achieve saturation, the biosorption remains stable since it was achieved an equilibrium state. High initial metallic concentration and high doses of biosorbent, increase the biosorption process due to the accessibility of the free sites (Bilal et al., 2018).

4. Adsorption process models

In this study, different kinetics and sorption equilibrium models were used. Since there is evidence that linearization may distort the estimate of model's parameter set (Largitte et al., 2016), all the kinetics results were fitted according to the nonlinear form of kinetic models by using Excel Solver and OriginPro8 program, except for some models which were more appropriate to analyse the results in linear form. The selection of the model which fits better the experimental data was based on statistical analysis, as detailed at the end of this section.

4.1 Adsorption kinetics

The study of the adsorption kinetics allows to understand the process of removing pollutants by adsorbents. From the kinetic parameters, information about the mass transfer and chemical/biochemical reaction are provided which help to model adsorption processes (Rangabhashiyam et al., 2019). In this section, adsorption kinetic models such as external mass transfer and intraparticle model (Crini et al., 2018; Weber; et al., 1962) and empirical kinetic models such as the pseudo-first order model, the pseudo-second order model and Elovich model (Ho et al., 1999; Lagergren, 1898; Low, 1960) will be presented.

4.1.1 Pseudo-first order model

Lagergren's first-order rate equation is considered non-reversible and based on the adsorption capacity rate which considers the proportion between the occupation of adsorption sites and unoccupied sites and is represented by Equation 4.1 (Lagergren, 1898),

$$q_{CAL} = q_{CAL,EQ} \cdot (1 - e^{-K_1 \cdot t}) \qquad \text{Equation 4.1}$$

where q_{CAL} ($\mu g_{FL}/g_{ALGAE}$) and $q_{CAL,EQ}$ ($\mu g_{FL}/g_{ALGAE}$) are the amount of adsorbate sorbed at time t (min) and at equilibrium, respectively, and K_1 (1/min) is the kinetic rate constant of pseudo-first order adsorption.

This model is founded in some assumptions such as (Lagergren, 1898):

- adsorption only occurs at specific sites and there is no interaction between adsorbed molecules;
- the adsorption energy is independent on the surface coverage;
- the maximum adsorption capacity corresponds to the saturation of adsorbate on the monolayer of the surface of the adsorbent;
- adsorbate concentration is constant.

According to Rangabhashiyam and Balasubramanian (2019), this model has greater importance only at the initial stage of the biosorption.

4.1.2 Pseudo-second order model

This model considers that the rate of occupation of adsorption sites is proportional to the square of the number of unoccupied sites, as represented by Equation 4.2 (Ho et al., 1999),

$$q_{CAL} = \frac{q_{CAL,EQ}^2 \cdot K_2 \cdot t}{1+q_{CAL,EQ} \cdot K_2 \cdot t} \quad \text{Equation 4.2}$$

where K_2 ($g_{ALGAE}/(\mu g_{FLX} \cdot min)$) is the equilibrium rate constant of pseudo-second order adsorption. This model is based on the same assumptions of pseudo-first order model, however, unlike the pseudo-first order model, this model is suitable for the entire range of the contact time (Ho et al., 1999).

4.1.3 Elovich's model

This model is based on the following assumptions(Low, 1960):

- adsorption energy increases linearly with the adsorbent surface coverage;
- the adsorbate concentration is constant;
- the adsorption process occurs only at specific sites and it is considered that even if there is an interaction between adsorbed molecules, it does not affect significantly the adsorption kinetics at low surface coverage.

The model is represented by Equation 4.3 (Low, 1960),

$$q_{CAL} = \frac{1}{\beta_E} \cdot ln\ (\alpha_E \cdot \beta_E) + \frac{1}{\beta_E} \cdot ln\ (t) \quad \text{Equation 4.3}$$

where α_E ($\mu g_{FLX}/(g_{ALGAE} \cdot min)$) is the initial adsorption rate constant of Elovich model and β_E ($g_{ALGAE}/\mu g_{FLX}$) represents the constant of desorption related to the extent of surface coverage and to the activation energy for chemisorption.

4.1.4 External mass transfer model

In the mass transfer models, diffusion of the adsorbate occurs in several steps: initially the adsorbate migrates from the bulk of the solution to the boundary film surrounding of the adsorbent surface; the molecules diffuse through the boundary layer to the surface of the adsorbent (external mass diffusion or film diffusion); then the adsorbate diffuses from the surface to the interior of the particle (pore diffusion or intraparticle diffusion); the final step is the attachment of the adsorbate molecules onto the material surface at the accessible sites. The third stage is the fastest between them, so the other ones are usually the limiting stages in the adsorption process rate (Crini et al., 2018).

For the external mass transfer model, boundary layer diffusion is the controlling resistance of the process. There is the transportation of the adsorbate molecules through the boundary layer and the thickness of this boundary depends on the stirring rate of the bulk solution. The thinner the boundary layer is, the higher the rate of the external diffusion (Crini et al., 2018).

The external mass transfer is given by Equation 4.4,

$$\frac{dC_{FLX}}{dt} = -K_{EXT} \cdot S_{EXT} \cdot (C_{FLX} - C_{FLX,EQ}) \quad \text{Equation 4.4}$$

where C_{FLX} ($\mu g_{FLX}/dm^3$) and $C_{FLX,EQ}$ ($\mu g_{FLX}/dm^3$) are the concentration of the fluoxetine at time t and at the equilibrium, respectively, K_{EXT} ($g_{ALGAE}/(dm^2 \cdot min)$) is the external mass transfer and S_{EXT} (dm^2/g_{ALGAE}) is the specific surface area.

The external mass diffusion occurs at the beginning of the adsorption process, so as t → 0, $C_{FLX,EQ}$ approaches 0, so Equation 4.4 is simplified to Equation 4.5 (Furusawa et al., 1973),

$$\left[\frac{dC_{FLX}}{dt}\right]_{t\to 0} = - K_{EXT} \cdot S_{EXT} \cdot C_{FLX} \qquad \text{Equation 4.5}$$

Hence, the external mass coefficient can be estimated from the slope at t=0 of a plot of LN ($C_{FLX}/C_{FLX,0}$) versus t.

Since the biomass has been introduced in a system as a cell suspension under with constant stirring, all points of the cells surface is available for binding with the pharmaceutical and the thickness of the boundary layer is neglectable. Therefore it is expected that the external resistance should be (Aksu, 2002; Largitte et al., 2016).

4.1.5 Intraparticle diffusion model

The intraparticle diffusion model assumes that the liming step to mass transfer resistance occurs after the adsorbate molecules have passed through the boundary layer and they are adsorbed in the pore's sites of the adsorbent (Weber; et al., 1962).

The form of the intraparticle diffusion model can be expressed as Equation 4.6 (Weber; et al., 1962),

$$q_{CAL} = K_{ID} \cdot t^{1/2} + C_{ID} \qquad \text{Equation 4.6}$$

where K_{ID} ($\mu g_{FLX}/(g_{ALGAE} \cdot min^{1/2})$) is the intraparticle diffusion rate constant and it is given by the slope of the plot q_{CAL} versus $t^{1/2}$. C_{ID} ($\mu g_{FLX}/g_{ALGAE}$) is the thickness of the boundary layer. The extension of the pore network and its tortuosity contribute to increase the internal resistance.

4.2 Adsorption isotherms

The adsorption isotherms are defined by constants related to surface properties and affinities of the biomass and allow to estimate the adsorption capacity of adsorbents (Aksu, 2002). Isotherms show the relation between the pollutant concentration in the equilibrium state and the amount of pollutant (adsorbate) adsorbed by unit mass of the biomass at a certain and constant temperature. Generally, adsorption process data was shown better fitting with isotherm models that use two and three parameters (Flory, 1953; Freundlich, 1906; Langmuir, 1918; Redlich et al., 1959; Sips, 1948; Tóth, 1971). In this section, the isotherm models of Langmuir, Freundlich, Sips, Redlich-Peterson, Tóth and Flory-Huggins will be presented.

4.2.1 Langmuir's model

The Langmuir model was defined on some assumptions such as (Langmuir, 1918):

- adsorption occurs on a homogenous monolayer surface;
- there is no adsorption in sites already occupied;
- all sites are considered similar and energetically identical;
- there is no interaction between adsorbed molecules;
- adsorption energy is constant;

- the greater the distance between adsorbent and adsorbate, the lower the strength of the intermolecular attractive forces;
- adsorption is limited by the uptake capacity.

Langmuir isotherm equation is applied for monolayer adsorption onto a surface with a finite number of particular sites and can be written as Equation 4.7 (Langmuir, 1918),

$$q_{CAL,EQ} = \frac{q_{MAX,L} \cdot K_L \cdot C_{FLX,EQ}}{1 + K_L \cdot C_{FLX,EQ}} \quad \text{Equation 4.7}$$

where $q_{MAX,L}$ ($\mu g_{FLX}/g_{ALGAE}$) indicates the maximum uptake capacity of the adsorbents, K_L ($L/\mu g_{FLX}$) is the Langmuir adsorption constant related to the affinity of the binding sites and $C_{FLX,EQ}$ ($\mu g_{FLX}/L$) represents the equilibrium adsorbate concentration. The value of q_{MAX} represents the limit of the experimental adsorption capacity when the surface is filled with the molecules and allows to evaluate the adsorption performance.

The Langmuir isotherm can be used to evaluate the affinity between adsorbate and adsorbent using the dimensionless separation factor (R_L) given as Equation 4.8,

$$R_L = \frac{1}{1 + K_L \cdot C_{FLX;0}} \quad \text{Equation 4.8}$$

where $C_{FLX,0}$ indicates the initial concentration of the adsorbate concentration ($\mu g_{FLX}/L$). If the R_L values are between 0 and 1 reflect favourable adsorption. For R_L values that are 0 or higher than 1, the adsorption is irreversible or unfavourable, respectively.

4.2.2 Freundlich's model

This is an empirical model that rests on non-ideal, reversible adsorption, infinite binding sites and extended to multilayer adsorption.

This model describes the heterogeneity of the adsorbents surface and the exponential distribution of active sites of adsorbents and their respective energies. It is based on the hypothesis that the sites with stronger bindings are those that are first occupied by adsorbate molecules and thus, as the occupation of the active sites increases, the binding strength declines. The Freundlich isotherm equation represented by Equation 4.9,

$$q_{CAL,EQ} = K_F \cdot C_{EQ}^{1/n_F} \quad \text{Equation 4.9}$$

where K_F ($(\mu g_{FLX}^{1-1/nF} \cdot L^{1/nF})/g_{ALGAE}$) is the Freundlich isotherm constant and n_F represents the Freundlich exponent, also called as adsorption intensity, which allows to obtain information about whether the process is favourable or not. In relation to the slope range, as values get close to zero, more heterogeneous is the surface of adsorbents contrary to the systems with slopes close to one. If it is below one, it means that is a chemisorption process and if $1/n_F$ value is above one, it is a cooperative adsorption process (Freundlich, 1906). Unlike the Langmuir model, the Freundlich model does not give information about the monolayer adsorption capacity (Aksu, 2002).

4.2.3 Sips' model

A mix of Langmuir and Freundlich models results in the Sips' model. When dealing with low concentrations of the adsorbate, the Sips isotherm model turns into the Freundlich's isotherm and at high concentrations, the model reduces to the Langmuir's isotherm. The simplified Sips' model is given by Equation 4.10 (Sips, 1948),

$$q_{CAL,EQ} = \frac{q_{MS} \cdot K_S \cdot C_{EQ}^{MS}}{1 + K_S \cdot C_{EQ}^{MS}} \qquad \text{Equation 4.10}$$

where q_{MS} ($\mu g_{FLX}/g_{ALGAE}$) is the Sips maximum adsorption capacity, K_S ($L^{1/MS}/\mu g_{FLX}^{1/MS}$) represents the Sips isotherm constant and MS is the Sips model exponent (from 0 to 1).

4.2.4 Redlich-Peterson's model

The three-parameter Redlich-Peterson isotherm model is an improvement of the features of Langmuir and Freundlich's models. This model is given by the Equation 4.11 (Redlich et al., 1959),

$$q_{CAL,EQ} = \frac{K_{RP} \cdot C_{EQ}}{1 + a_{RP} \cdot C_{EQ}^{\beta_{RP}}} \qquad \text{Equation 4.11}$$

where K_{RP} (L/g_{ALGAE}) and a_{RP} $(L/\mu g_{FLX})^{\beta RP}$ are Redlich-Peterson model parameters. β_{RP} is an exponential value that goes from 0 to 1. If β_{RP} equals to 1, then Equation 4.11 becomes the Langmuir's equation and if β equals to 0, the Redlich-Peterson isotherm model turns into Freundlich's equation.

4.2.5 Tóth's model

Tóth's model is based on the Langmuir model and shows a satisfactory fitting to heterogeneous and multilayer adsorption systems. It is expressed by Equation 4.12,

$$q_{CAL,EQ} = \frac{K_T \cdot C_{EQ} \cdot Q_{MAX,T}}{\left[1 + (K_T \cdot C_{EQ})^{n_T}\right]^{1/n_T}} \qquad \text{Equation 4.12}$$

where $q_{MAX,T}$ ($\mu g_{FLX}/g_{ALGAE}$) indicates the maximum uptake capacity of the adsorbents, K_T ($L/\mu g_{FLX}$) is Tóth isotherm constant and n_T is Tóth isotherm exponent. If n_T=1, Equation 4.12 converts into the Langmuir's isotherm. The system is classified as heterogeneous, if the n_T value is higher than 1 (Tóth, 1971).

4.2.6 Flory-Huggins' model

The Flory-Huggins' isotherm shows the degree of surface coverage of an adsorbate on the adsorbent which allows to verify the feasibility and spontaneous nature of the process. The isotherm is given by Equation 4.13 (Flory, 1953),

$$\frac{\theta}{C_{FLX,0}} = K_{FH} \cdot (1 - \theta)^{n_{FH}} \qquad \text{Equation 4.13}$$

where θ is the degree of the surface coverage, K_{FH} ($L/\mu g_{FLX}$) represents the Flory-Huggins equilibrium constant and n_{FH} is the model exponent. The degree of surface coverage is given using Equation 4.14,

$$\theta = 1 - \frac{C_{FLX,EQ}}{C_{FLX,\,0}} \qquad \text{Equation 4.14}$$

4.3 Statistical analysis

Conversion of the experimental data from non-linear to linear regression adds and changes the error structure of the data and for this reason, non-linear regressions become a better option to analyse data. In the case of non-linear regressions, these normally require error minimization between experimental and predicted data by the models, based on convergence criterion (Kumar et al., 2008).

In the present study, the statistical analysis of the fitted models was based on the following parameters: coefficient of determination (R^2); sum of the square of the errors (SSE); chi-squared test (X^2); chi-squared reduced test (X^2_{red}) and standard error of estimate ($S_{y.x}$).

4.3.1 Sum of squares of the errors

The sum of squares of the errors (SSE) can be defined by Equation 4.15 (Kumar et al., 2008),

$$SSE = \sum (q_{EXP} - q_{CAL})^2 \qquad \text{Equation 4.15}$$

and it is the sum of the squares of the difference between experimental (q_{EXP}) and calculated by values by the models (q_{CAL}).

4.3.2 Standard error of estimate

Standard error of estimate ($S_{y.x}$) considers the number of experimental values comparing with the number of model parameters, thus defines the reliability of the respective model to express the experimental data. The lower $S_{y.x}$ values, the better is the fitting of the model. This parameter is represented by Equation 4.16 (Al-Muhtaseb et al., 2011),

$$S_{y.x} = \sqrt{\frac{\sum (q_{EXP} - q_{CAL})^2}{d.f.}} \qquad \text{Equation 4.16}$$

where the degrees of freedom (d.f.) is given by the subtraction (n-p), being n the number of experimental data and p the number of model parameters.

4.3.3 Coefficient of determination (Adjusted)

The coefficient of determination represents the percentage of the variance of the mean and is used to analyse the fitting degree of the models to the experimental data. It is defined by Equation 4.17 (Largitte et al., 2016),

$$R^2 = 1 - \frac{\sum (q_{EXP} - q_{CAL})^2}{\sum (q_{EXP} - q_{EXP,AVG})^2} \qquad \text{Equation 4.17}$$

where q_{EXP} ($\mu g_{FLX}/g_{ALGAE}$) is the experimental determined capacity of adsorption of adsorbent, $q_{EXP,AVG}$ is the mean of the experimental determined capacity of adsorption of adsorbent

($\mu g_{FLX}/g_{ALGAE}$) and q_{CAL} ($\mu g_{FLX}/g_{ALGAE}$) is the capacity of adsorption of adsorbent calculated from one of the models.

The number of parameters can interfere in the over-fitting of R^2, if the sample size is relatively small. The amount of samples should be much larger than the number of parameters in order to provide a good estimate of its population value (Millsap et al., 2009). R^2_{adj} is given by Equation 4.18,

$$R^2_{adj} = 1 - \frac{n-1}{n-p} \times (1 - R^2) \qquad \text{Equation 4.18}$$

4.3.4 Non-linear chi-square test (Reduced)

This parameter, non-linear chi-square test (X^2), can be calculated by the sum of the squares of the differences between experimental and calculated data from models, with each squared difference divided by the corresponding data values from models. It is represented by Equation 4.19 (Chen et al., 2008),

$$X^2 = \sum \frac{(q_{EXP} - q_{CAL})^2}{q_{EXP}} \qquad \text{Equation 4.19}$$

Reduced chi-square test (X^2_{red}) is advisable to use instead of X^2 for model comparison and it is represented by Equation 4.20 (Spiess et al., 2010),

$$X^2_{red} = \frac{\sum (q_{EXP} - q_{CAL})^2}{d.f.} \qquad \text{Equation 4.20}$$

X^2_{red} values close to one, represent a good approximation of the fitting function to the experimental function. If the reduced chi-square is much higher than one, it means that the model shows an unsuitable fitting.

4.3.5 Fisher Test

Fisher test is a statistical method that evaluates the models fitting to the experimental data, providing the best fit model. F-test is based on the coefficient of variances of two different models (F_{calc}) and verifies if this difference is significant. For that F_{calc} is compared with a tabulated value of the Fisher distribution, called critical F, ($F_{\alpha,d.f._1,d.f._2}$). $F_{\alpha,d.f._1,d.f._2}$ is obtained from the number of degrees of freedom and the level of significance that are found in Fisher distribution (Archangel'skij, 2013). The 95% confidence interval was chosen for this test, therefore, α was equal to 0.05 (Montgomery et al., 2011). The model with the best fit is the one that shows the smallest variance and is placed in the numerator as the reference model. If $F_{calc} < F_{\alpha,d.f._1,d.f._2}$, there is no statistical difference between models, and therefore no evidence that the reference model is more adequate to define the experimental data (Archangel'skij, 2013). The F_{calc} value was calculated by Equation 4.21,

$$F_{calc} = \frac{\frac{SSE_{ref}}{d.f._{ref}}}{\frac{SSE}{d.f.}} \qquad \text{Equation 4.21}$$

4.3.6 Akaike information and Bayesian information criterions

The Akaike information criterion (AIC) is also a statistical method that evaluates the loss of information in the process of adjusting the model to the experimental data. The lower is the AIC, the less information is lost (Millsap et al., 2009). The AIC is given by Equation 4.22 (Martcheva, 2015),

$$AIC = n \times LN\left(\frac{SSE}{n}\right) + 2 \times p \qquad \text{Equation 4.22}$$

AIC is calculated from SSE and p values, for this reason, a decrease in SSE, which means a better fit, will necessarily decrease the AIC value. A larger number of parameters, which translates into a greater complexity of the model, will correspond to an increase in the AIC and a worse adjustment of the model (Millsap et al., 2009). Therefore, AIC penalizes models with too many parameters e discourages overfitting (Martcheva, 2015).

Bayesian information criterion (BIC) is a version of AIC, however, BIC takes a higher penalty for the number of parameters and is given by Equation 4.23,

$$BIC = n \times LN\left(\frac{SSE}{n}\right) + p \times LN(n) \qquad \text{Equation 4.23}$$

5. Experimental description

5.1 Materials

5.1.1 Pharmaceutical

In the present study, a widely consumed pharmaceutical, fluoxetine, was selected as the adsorbate. This pharmaceutical is prescribed to treat depression due to its ability to inhibit serotonin reabsorption which leads to an increase of the extracellular level of serotonin in the synapse. Serotonin is a neurotransmitter that affects psychological and biological tasks as mood, appetite, sleep, memory and sexual function. In recent studies, fluoxetine hydrochloride has been studied to treat bulimia and severe obesity (Ravishankar et al., 2016).

This pharmaceutical was purchased as fluoxetine hydrochloride (Figure 5.1), $C_{17}H_{18}F_3NO{\cdot}HCl$, CAS number 56296-78-7 (>98%, Merck KGaA, USA).

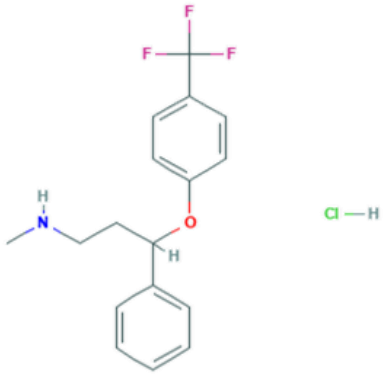

Figure 5.1. Chemical structure of fluoxetine hydrochloride (PubChem, 2019b).

Some of the physical and chemical proprieties are shown in Table 5.1**Error! Reference source not found.**.

Table 5.1. Physical and chemical proprieties of pharmaceutical fluoxetine hydrochloride

Proprieties	Fluoxetine hydrochloride
Chemical name	d,1-N-methyl-3-phenyl-3-[(α,α,α-trifluoro-p-tolyl)oxy] propaylamine hydrochloride (Santa Cruz Biotechnology, 2019)
Molecular weight	345.79 g/mol (Santa Cruz Biotechnology, 2019)
CAS	56296-78-7 (Santa Cruz Biotechnology, 2019)
Physical description	White to off-white, crystalline, without odour, solid (Florey, 1990)
Melting range	158 - 159ºC (Merck KGaA, 2019)
Solubility	4 mg/mL in water; >5 mg/mL in dimethyl sulfoxide; 100 mg/mL in methanol (Merck KGaA, 2019)
Partition coefficient: n-octanol/water (Log Pow)	1.8 at 25 °C (Merck KGaA, 2019)
Acidity constant (pKa)	9.8 (DrugBank, 2019)

The acid dissociation constant, pKa, is an important parameter in the biosorption process since this evaluates the extent of ionization of fluoxetine as a function of the solution pH. Components charge may change depending on the solution's pH and compound's pKa. Fluoxetine hydrochloride can be classified as a weak base since pKa is 9.8. Therefore, for conditions considered normal for residual water (pH 7-8) (Guldhe et al., 2017), fluoxetine will be mainly protonated and above 9.8, molecules demonstrated a negative charge.

5.1.2 Microalgae

The freshwater microalga *Chlorella vulgaris*, Ref. 211-8L from SAG was selected as biosorbent for this study. Inoculum for the experiments was cultivated in sterilised Erlenmeyer flasks with cap (made with sterile carded cotton stoppers and gauze and finally aluminium foil) in OECD (2011) standard culture medium described in Section 5.1.3. All manipulations of the algae were made inside a laminar flow cabinet (Faster, two 30 models, Italy) to avoid microalgae contamination by other microorganisms,

Microalgae were kept in a room under controlled constant conditions, at 22±2ºC via air conditioning (Sanyo, Q105ASP01) and under light provided by four fluorescent lamps that generate universal white light (Osram, L36W/ 865, Germany).

In order to increase the cell growth in cultures agitation by air bubbling was used as showed in Figure 5.2. The agitation of test flasks was performed by an orbital agitator (Bunsen, AO-400).

In order to study the effect of algae metabolism in the biosorption process, in addition, to live microalgae, dead microalgae were used for comparison. To obtain dead biomass, microalgae were frozen at -80ºC and then submitted to lyophilization process (slow freeze-drying) in a freeze-drier (Inficon, PGD400 model) for 3 days at -44ºC and 0.7 mbar.

Figure 5.2. Growth of *Chlorella vulgaris* under controlled conditions.

5.1.3 Culture medium

The purpose of the growth medium is to provide the substrate to microalgae growth. There are several growth media but for this project, it was used OECD TG 201 medium which is according to test nº201 Guidelines for the Testing of Chemical, Freshwater Alga and

Cyanobacteria Growth Inhibition Test (OECD, 2011). This guideline was established by European Parliament and Council on the Registration, Evaluation, Authorisation and Restriction of Chemicals (REACH) and is described in Regulation (EC) 440/2008 of 30 May 2008 in accordance with Regulation (EC) 1907/2006. The composition of OECD TG 201 medium is described in Table 5. 2:

Table 5. 2. Concentration of nutrients in the medium growth from Regulation (EC) 440/2008 (OECD, 2011).

Backup solution	Component	Concentration backup solution (g/L)	Concentration medium (mg/L)
1	NH_4Cl (99.80%, Merck KGaA)	1.5	15.0
	$MgCl_2 \cdot 6(H_2O)$ (99%, BDH)	1.2	12.0
	$CaCl_2 \cdot 2(H_2O)$ (for analysis, Merck KGaA)	1.8	18.0
	$MgSO_4 \cdot 7(H_2O)$ (for analysis, LabChem)	1.5	15.0
	$KH_2 \cdot PO_4$ (for analysis, LabChem)	0.16	1.6
2	$FeCl_3 \cdot 6(H_2O)$ (99%, Sigma-Aldrich)	0.064	0.064
	$Na_2EDTA \cdot 2(H_2O)$ (≥99.0%, Fluka)	0.1	0.1
3	H_3BO_3 (100.30%, Merck KGaA)	0.185	0.185
	$MnCl_2 \cdot 4(H_2O)$ (>99%, Fluka)	0.415	0.415
	$ZnCl_2$ (98%, Merck KGaA)	0.003	0.003
	$CoCl_2 \cdot 6(H_2O)$ (Sigma-Aldrich)	0.0015	0.0015
	$CuCl_2 \cdot 2(H_2O)$ (99.999%, Sigma-Aldrich)	0.00001	0.00001
	$Na_2MoO_4 \cdot 2(H_2O)$ (99.50%, Merck KGaA)	0.007	0.007
4	$NaHCO_3$ (99.50%, Riedel-de-Haën)	50.0	50.0

For the preparation of OECD medium, it was prepared previously four backup solutions, one solution with macronutrients (solution 1) and three solutions with micronutrients (solutions 2 to 4). For one litre of the growth medium, it was added 10 mL of backup solution 1 and 1 mL of backup solutions 2, 3 and 4.

To preparation the solutions, it was used deionized water treated by a Millipore deionizer (Helix 3 model, France) and sterilized in an autoclave (AJC, uniclave 88 models, Portugal), at 121ºC, for 20 min, to ensure aseptic conditions. All backup solutions were sterilized in an

autoclave as well, however before sterilization, backup solution four was filtered on a 0.47 µm diameter pore cellulose membrane filter (GN-6 metricel®, PALL Gelman, USA) since high temperature, as the one reached inside the autoclave, can cause sodium hydrogen carbonate precipitation.

While backup solutions were not used, they were stored at 4ºC in a fridge (Liebherr) and without light exposure to avoid degradation.

The preparation of the culture medium was prepared in a laminar flow cabinet in order to avoid contamination by microorganisms.

5.2 Methods

5.2.1 Quantification of fluoxetine

For the quantification of the pharmaceutical fluoxetine, an HPLC-FLD (Shimadzu Corporation, Japan) (Figure 5. 3) equipped with a 20AB LC pump, a DGU-20A5 degasser, a CTO-20AC column oven, a SIL 20A automatic injector, and a RF-10AXL fluorescence detector (FLD) was used. HPLC-FLD analysis was performed on a Luna C18 chromatographic column (4.6 × 150 mm, 5 µm particle size, Phenomenex, USA). A 0.1% formic acid solution in ultrapure water (eluent A) and acetonitrile (eluent B) were the eluents used in the mobile phase. Chromatographic program starts with a gradient from 10 to 100% (eluent B) in 5 min, held in 100% (eluent B) for 4 minutes, then eluent B decreased from 100% to 10% in 1 minute and held for 6 minutes at 10% (eluent B). The total time for completing the chromatographic run was with 16 minutes. The flow rate of mobile phase was set to 1.0 mL/min and the injection volume of 20 µL was used. Fluorescence detection was performed at the excitation wavelength of 230 nm and at the emission wavelength of 290 nm. Data acquisition was performed using LCsolution software (Shimadzu Corporation, Japan).

Figure 5. 3. HPLC-FLD equipment.

5.2.2 Quantification of algae biomass

There are multiple methods to quantify microalgal biomass, such as direct cell counting, measurement of optical density by spectrophotometer, algal biomass by weighting and chlorophyll *a* content measurement, among others. Cell counting method is considered the most precise method, in addition to being laborious, cannot be applied to all cases, e.g. agglomerate microalgae. In general, dry weight and ash-free dry weight are also very reliable methods for microalgal biomass quantification but once again it is a time consuming task. By optical density, also known as absorbance or turbidity, is not so accurate since cell morphology and composition can change, even the medium may create variations, however, it is a simpler, faster and non-destructive method (Griffiths et al., 2011; Lu et al., 2017).

For absorbance, the wavelength used is where there is maximum absorbance corresponding to the range with more sensitivity. Pigments are some of the constituents of microalgae that consist mostly in chlorophylls and carotenoids that absorb in a specific region of the light spectrum. Chlorophyll *a* is the major pigment in most microalgal cells. It is expected to find an association between the largest signal and the wavelength with a maximum absorbance of the pigment, however in this same range, if the pigment content changes, it may be associated the largest error as well. For the species *Chlorella vulgaris,* there is maximum absorbance in regions of 440, 480 and 680 nm, however, according to Griffiths *et al.* (2011), at 680 nm, absorbance per unit of biomass changes over a normal microalgal growth cycle due to the change of pigment content of the cells. This can be minimized by using a wavelength that is outside of the range of pigment absorption, such as at 750 nm, which is used in several studies (U.S. Environmental Protection Agency, 2002).

Chlorophyll *a* fluorescence measurement is also a fast-used method to determine microalgae biomass since there is a good linear relationship between microalgal cellular densities and fluorometric values (U.S. Environmental Protection Agency, 2002). The fluorescent spectral scans in algal cultures showed significant excitation and emission peaks that correspond to chlorophyll *a* fluorescence peaks. It was found an excitation peak at 434 nm and an emission peak at 684 nm (Held, 2011; Zhao et al., 2018). Therefore, to measure the fluorescence intensity, it was selected a filter set of an excitation filter that transmits 485/20 nm light and an emission filter that transmits 645/40 nm light and posteriorly, related to dry weight of microalgae. To quantify absorbance and fluorescence of chlorophyll a ($FI_{485/645}$), microplate reader (BioTek, Synergy HT, USA) using 96-well transparent and other non-transparent polystyrene microplates, respectively. For dead microalgae, absorbance measurement could be used, however, it was chosen a more direct way, weigh it. For live microalgae, it was opted to use fluorescence instead of absorbance since a better correlation coefficient was achieved between fluorescence and biomass concentration (C_{ALGAE}).

For dry weight quantification, 47 mm glass microfiber filters (Whatman, Grade 934-AH, UK) were prepared prior to be used by filtering around 60 mL of deionized water and then dried in an oven (Selecta P, 2000208, E.U.) at 70ºC for 24 h. After dried and weighted up, a rigorous volume

(10 or 20 mL) of culture was filtered through the previously prepared filters. The filtrates were dried in the oven at 70ºC for 24 h and weighed again. All dry weight measurements were carried out in duplicate.

5.2.3 Microalgae characterization

5.2.3.1 FTIR characterization

Fourier-transform infrared spectroscopy (FTIR) characterization was procedure. Firstly, a mixture of dried live and lyophilized microalgae was diluted in KBr (20 mg of sample ground with 200 mg of KBr) and then pressed into pellets by using a manual hydraulic pellet press. Infrared spectra were recorded in the range of 400-4000 cm^{-1} with 2 cm^{-1} resolution, using transmittance technique (Nicolet 6700 FT-IR, MCT/A detector; Thermo Scientific, USA). Results were analysed in OMNIC Spectra 7.3 software. This procedure was applied to samples of live and lyophilized microalgae, with and without being in contact with fluoxetine solution (~50 μg_{FLX}/L). Then, these samples were dried at room temperature for 4 days.

5.2.3.2 Determination of point zero charge

Factors such as ionic speciation, microalgae medium conditions, the medium pH, the structure of the microbial layers, physiological state of the cell and others can influence biosorption process (Andrès et al., 2000). The cell surface shows a charge due to surface functional groups such as -COOH, -OH, $-NH_2$ and others from cell walls, extracellular polysaccharides and other materials (Cho et al., 1994). Thus, the surface cell can demonstrate amphoteric behaviour, negative or positive charge, depending on the pH and this tendency can be evaluated through the determination of the pH at point of zero charge (PZC). The PZC defines the conditions in which the surface charge is zero, meaning that the amount of negative charge and positive charge are equal. This point is a pH value since it is a pH-dependent surface charging (Kosmulski, 2009). For pH values that are below the pH_{PZC} value, the surface is protonated due to the biosorption of protons from the solution and partial complexation of electrolyte (H_3O^+) and for this reason, the surface will show a higher tendency to adsorb anions (Silva et al., 2019).

In this project, the point of zero charge (pH_{PZC}) was determined according to the method proposed by Rivera-Utrilla et al (2001). For live microalgae, the volume of algae was determined in order to obtain 50 mg portions and for lyophilized *Chlorella vulgaris*, 50 mg portions were weighted and posteriorly, placed in Erlenmeyer flasks and mixed with 50 mL of NaCl 0.01 M and then pH was adjusted in order to study the range between 3 and 11 ($pH_{INITIAL}$). The pH was adjusted with NaOH or HCl solution with concentrations from 0.01 to 1 M. Samples were stirred using a magnetic stirrer (VELP Scientifica, F203A0178, EU) at 400 rpm during 24 h. For live microalgae, samples were stirred within a spot with no light to prevent algae growth. The final pH was recorded (pH_{FINAL}) using a pH meter (Consort, model C861). The pH_{FIN} was plotted against ΔpH, the point at which the curve crossed in the x-line was took as the pH_{PZC}.

5.2.3.3 Study of pH influence

In order to study the effect of pH over the biosorption process, 20 mL of ultrapure water obtained by a Millipore Sustemand 50 mg microalgae portions were mixed using a magnetic stirrer (VELP Scientifica, F203A0178, EU) for 1 h in Erlenmeyer flasks. Then the pH adjustment was performed with HCl or NaOH (0.1 and 0.01 M) in order to obtain values in the range between 5 and 10. A defined volume of pharmaceutical solution was added, and all solution volumes were adjusted to 25 mL to obtain a final concentration of 500 μg_{FLX}/L. The initial pH value ($pH_{INITIAL}$) was measured and recorded using a pH meter (Consort, model C861). All the solutions were stirred for 180 min at 400 rpm. The pH was measured again at the end of the experiment (pH_{FINAL}). Samples of 1 mL were withdrawn to 1.5 mL Eppendorf tubes and centrifugated (Heraeus, Fresco 21, Germany) at 5000 rpm for 5 min, the supernatants were collected and transferred to vials and then stored in the freezer to be analysed by High Performance Liquid Chromatography with a fluorescence detector, as described in section 5.2.6. A blank test for each pH was performed and consisted of repeating the experiments without the microalgae.

5.2.4 Kinetic studies

Experiments were carried out to study the biosorption kinetics of fluoxetine onto *Chlorella vulgaris.* The experiments were performed at room temperature (20-24°C) for 2 h.

From the microalgae culture, 45 mL was withdrawn and centrifuged at 8000 rpm for 10 min (Thermo Scientific, Heraeus Megafuge 16R, Germany), while 10.00 mL of the same culture was used for the determination of biomass through a filtration. After centrifugation, the supernatant was discarded, and the microalgae were added to the fluoxetine hydrochloride solution (Figure 5.4), this being the initial time of the kinetics test. The pharmaceutical solution with a 0.56 mg_{FLX}/L concentration was previously placed into a 250 mL flask before adding the microalgae then it was stirred at 500 rpm (SBS, ACS-160 model). The time was recorded, and the pH was measured continuously with a pH-meter (Consort, model C861) and pH electrode from VWR, model DJ113. Over the course of the experiment, 1 mL samples were withdrawn to 1.5 mL Eppendorf tubes and in the first 10 min, samples were withdrawn every 2 min; from 10 to 30 min, every 5 min; up to 1 h of analyse was withdrawn every 10 min and until the end of the experiment, samples were withdrawn every 20 min. In order to check whether Eppendorf material absorbed fluoxetine, one sample was taken directly into one amber vial and another into an Eppendorf and the concentration in the latest was lower about 0-10% than in the vial, hence Eppendorf plastic material could adsorb a small amount of pharmaceutical. Thus, for trials done ahead, the initial concentration was determined after being in the Eppendorf. All samples were centrifuged at 5000 rpm for 5 min (Heraeus, Fresco 21, Germany), the supernatants were collected respectively in amber vials and stored in the freezer (Liebherr) at 0°C to be analysed by High Performance Liquid Chromatography with fluorescence detector (HPLC-FLD, Shimadzu Corporation, Japan), as described in section 5.2.6.

To study the kinetic for dead cells, it was made the same procedure of the live cells, but in this case lyophilized microalgae were simply weighted and added to the fluoxetine hydrochloride solution. The initial lyophilized microalgae concentration was 137.16 mg_{FLX}/L. Thus, it was weighted rigorously 34.29 mg of biomass in a balance (Metter Toledo, NewClassic MS).

Figure 5.4. Kinetic analyse set-up.

The experimental biosorption capacities were calculated according to Equation 5.1.,

$$q_{EXP} = \frac{(C_{FLX,\ 0} - C_{FLX})}{m_{ALGAE}} \times V_{SOL} \qquad \text{Equation 5.1.}$$

where $C_{FLX,0}$ (μg_{FLX}/L) is the initial concentration of fluoxetine, C_{FLX} (μg_{FLX}/L) is the concentration of fluoxetine at a given time, t (min). V_{SOL} (L) is the solution volume and m_{ALGAE} (g_{ALGAE}) is the mass of adsorbent.

5.2.5 Equilibrium studies

For the equilibrium isotherm determination, the same initial fluoxetine concentration was used for all flasks and the initial biomass concentration was varied. For the live microalgae experimental, the volume of the culture of microalgae to be removed was determined previously in order to obtain different weights: 0.5, 1, 2, 7, 15, 30, 50, 70, 100 and 120 mg C*hlorella vulgaris*. Thereafter, the samples with the different volumes were centrifuged at 8000 rpm for 10 min and the supernatants were discarded. In Erlenmeyer's flasks with 25 mL of fluoxetine solution (~561 μg_{FLX}/L), previously collected biomasses were added, and the assay started. They were kept under continuous stirring on a stirring plate (VELP Scientifica, F203A0178, EU) at room temperature until equilibrium was reached (2 h), then 1 mL samples were withdrawn to 1.5 mL Eppendorf tubes (Figure 5.5) and were centrifuged at 5000 rpm for 5 min, and finally the supernatants were collected in vials and stored in the freezer at 0°C to be analysed by HPLC-FLD. Every sample was homogenous in a vortex (VWR, analogue vortex mixer 230V, USA) before being analysed on HPLC-FLD (section 5.2.6).

In the case of lyophilized biomass, the same portions as live microalgae, were rigorously weighed and then they experienced the same process of live microalgae.

Figure 5.5. Equilibrium analyse set-up.

6. Results and discussion

6.1 Quantification of algae and pharmaceutical

To quantify live microalgae, a calibration curve relating concentration and fluorescence was performed. The calibration curve was plotted for low and high sample concentration: low concentration range of [0-0.143] g_{ALGAE}/L and high concentration range of [0.381-1.016] g_{ALGAE}/L, thus, the experimental results were within the range of calibration curve concentrations. The relation between biomass dry weight (C_{ALGAE}) and $FI_{485/645}$ (Figure A. 1) were determined and is shown in Appendix A.

For the quantification of fluoxetine, retention time was compared with a standard solution and for its quantification, and a calibration curve was made in the range 1-2000 μg_{FLX}/L (with R^2>0.999). Deionised water was used to prepare the standards used in the calibration curve. The chromatogram of the 2 mg/L fluoxetine standard solution is shown in Figure B. 1 (Appendix B). The relations between areas (Peak Area) and fluoxetine concentration (C_{FLX}) were determined and is shown in Appendix B (Figure B. 2).

6.2 Characterization of *Chlorella vulgaris* microalgae

6.2.1 Sorbent characterization by FTIR

Microalgae cell walls include several compounds such as polysaccharides, proteins, lipids and other components which contain functional groups, such as, amino, amine, hydroxyl, imidazole, phosphate and sulphate (Crist et al., 1981), that may act as binding sites allowing biosorption of several pollutants (Hom-Diaz et al., 2017; Tam et al., 2002). Proteins are a major component in the microalgae composition, 42- 58% of biomass dry weight and around 20% of total proteins are assured to the cell wall. In *Chlorella vulgaris* species, lipids can be also found in the cell wall and on membranes of organelles and can reach 5-40% lipids per dry weight of biomass. The cell wall is a remarkable barrier also composed by carbohydrates, such as cellulose and starch (Safi et al., 2019).

Functional groups were identified in the microalgae by some bands of the infrared spectrum. Changes in the characteristics of the microalgae due to the application of the lyophilization process and to the contact with fluoxetine were searched by identification of functional groups in the FTIR spectra. A colour change was noticed in the samples where algae contacted with fluoxetine for 4 days. By observing Table 6.1, the pellets that contained only microalgae (a and c) showed green colour, characteristic from chlorophyll, while in those which contacted with fluoxetine (b and d), changed to a brown and light brown colour, respectively. Colour's samples corresponded to the

Table 6.1. Pellets to FTIR analyse: live microalgae; live microalgae with fluoxetine; lyophilized microalgae; lyophilized microalgae with fluoxetine.

	Without fluoxetine	**With fluoxetine**
Live microalgae		
Lyophilized microalgae		

Even at low concentrations, fluoxetine was already reported as a toxic compound for algal species. El-Bassat et al. (2012) concluded that fluoxetine, aside from affecting negatively cell growth as it was reported in the green alga, *P. subcapitata*, it may also cause cell rupture and cell deformations. Oxidative stress by pharmaceuticals was already reported in some algal species. Due to bioaccumulation of drugs, cells suffer an inhibition of the antioxidant enzyme activity, that are responsible to defend from high levels of ROS (reactive oxygen species), which allows a generation of ROS in excess and consequently, molecular damage (El-Bassat et al., 2012) due to several damage of cellular components and increase rate of mutagenesis (Kumar et al., 2016). Oxidative stress could be the reason for the colour modification, due to fluoxetine toxicity and its bioaccumulation. However, it should be noted that this would only explain the change in living algae since, in dead algae, its metabolism is no longer functioning and hence the generation of ROS. In lyophilized algae, the colour change occurs due to other phenomena (non-metabolic).

The IV spectrums can be seen in Figure 6.1, where 13 main bands were identified over the wavenumber range 450 to 3900 cm^{-1}.

The spectra of the live and lyophilized microalgae that had contact with fluoxetine and the spectrum of lyophilized microalgae were very similar which bands had slight between spectra. A broad and strong band 1 with a peak around 3400 cm^{-1} matches to the overlapping of stretching vibrations of functional groups O-H (vibration in water) and N-H groups of carbohydrates and proteins (Silva et al., 2019; Xie et al., 2014). Between 2850 and 2950 cm^{-1}, the bands 2 and 3 observed and are due to asymmetric and symmetric C-H stretching vibration of $-CH_3$/$-CH_2-$ groups, which are characteristic of lipids and fatty acids spectra (Driver et al., 2015; Xie et al., 2014). At ~1730 cm^{-1} (band 4), there is a peak that results from C=O stretching vibration of the ester group, also characteristic of lipids and fatty acids spectra (Hadjoudja et al., 2010; Xie et al., 2014). Two stronger peaks between 1640 and 1550 cm^{-1} (band 5 and 6) are due to stretching vibrations C=O of amide I and N-H bending of amide II vibrational modes of proteins, respectively (Xie et al., 2014). The band 7 observed at 1460 cm^{-1} may result from asymmetric bending of CH_3 and CH_2 of proteins or lipids (Silva et al., 2019). The band 8 (~1380 cm^{-1}) could be assigned to asymmetric bending of CH_3 and CH_2 of proteins and to symmetric stretching of C-O in carboxylic

acids (Silva et al., 2019; Udoh et al., 2012). The band at 1300 cm^{-1} (band 9) was associated with stretching vibrations of P=O from nucleic acid and other compounds containing phosphate (Udoh et al., 2012). In the spectral region from 900 to 1200 cm^{-1}, there are several peaks which correspond to the stretching C-OH and C-O-C vibrations of polysaccharides from carbohydrate absorption bands at 1190, 1116, 1066 and 1056cm^{-1} (band 10 to 13) in live microalgae without being in contact with fluoxetine. Beyond these functional groups, they correspond to symmetric stretching vibrations of phosphate functional groups (P=O) related to nucleic acid components (Hadjoudja et al., 2010; Xie et al., 2014). Proteins, carbohydrates, lipids and nucleic acids were the most dominant groups in the IV spectrum as the literature suggested.

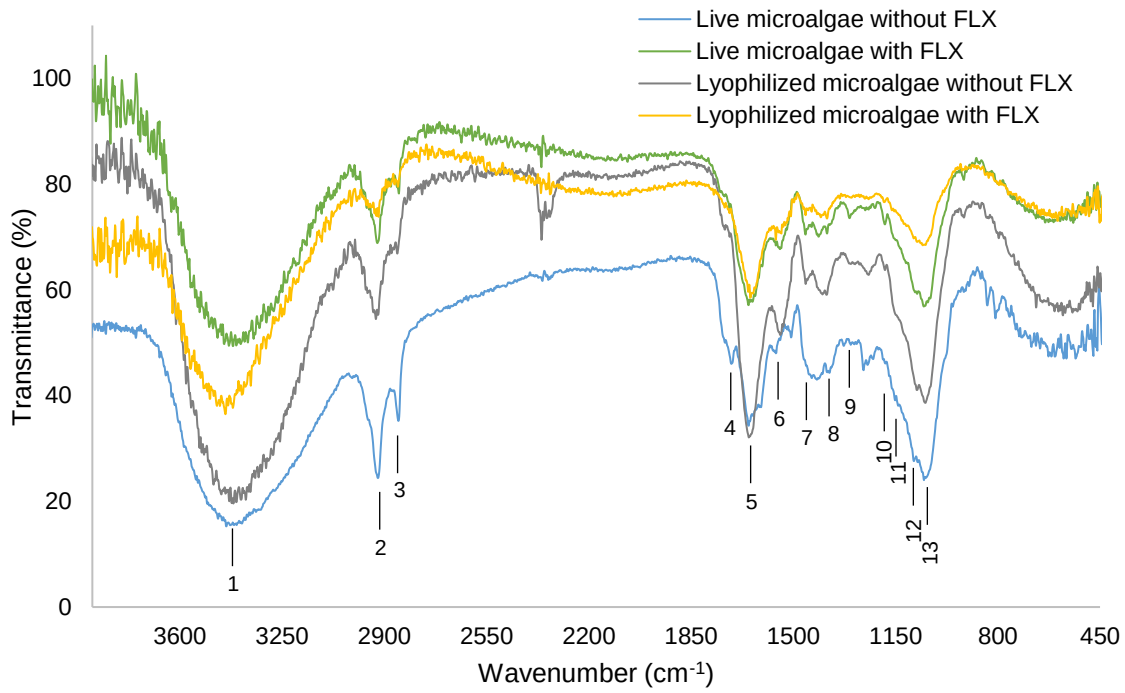

Figure 6.1. Infrared transmittance spectra of live and lyophilized Chlorella vulgaris with and without fluoxetine

Since chlorophyll *a* is a major component present in the microalgae and its structure is $C_{55}H_{72}O_5N_4Mg$ (Figure 6.2), it was expected to find in the spectra, the functional groups C-H, C-O, C=O and N-H. But functional groups as Mg-N, C-C and C=C were not found because they have low polarity or its amount was not enough to be detected by the spectrophotometer. The similarity between spectra also showed that lyophilization does not originate modifications in the chemical structure of the microalga *Chlorella vulgaris* as the literature proposed. According to (Chen et al., 2015), freeze-drying is a method to dry algae. Due to the development of ice crystals during the slow freezing process and sublimation afterwards in the lyophilization, the cell walls may obtain more pores without disrupting and therefore walls develop more permeability (Serra, 2015). However, if samples were frozen slowly, larger intracellular ice crystals may form and lead to disruption of the cell wall. In any way, this method allows to preserve the cell constituents or without varying the composition significantly (Chen et al., 2015).

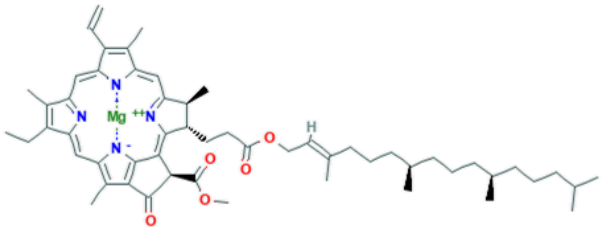

Figure 6.2. Chlorophyll *a* structure (Adapted from PubChem, 2019)

The FTIR spectra do not reveal a significant difference between freeze-dried and live *C. vulgaris*. The contact of the fluoxetine with the microalgae did not cause differences in the spectrum as well. This may be related to the low amount of fluoxetine contained in the samples that make it not detectable by the equipment or by the overlapping of other stronger bands in the same wavenumbers. In order to confirm this observation, a higher concentration of fluoxetine should be applied prior to FTIR analysis.

6.2.2 Point of zero charge

In the case of live microalgae, the pH_{PZC} obtained was 7.0 (Figure 6.3). At pH values of the solution below pH_{PZC}, the adsorbent surface acquires a positive charge due to the dissociated groups detected at FTIR, as carboxyl and hydroxyl present in the cell walls, while at pH of the solutions above pH_{PZC} value, the adsorbent surface tends to be negatively charged. Through the obtained information was not possible to identify the nature of the surface complexes involved in the solid surface, however, Silva et al. (2019) stated that biosorption of protons from the solution and partial complexation of electrolyte were possible processes responsible for the existence of charge. The mechanism involves an electrical double layer that is generated by a distribution of ions from the solution nearby, producing a charged surface. Electrical double layer, with a negative charge, includes the charged surface and excess of counterions in the solution (Silva et al., 2019). As mentioned before, pKa of hydrochloride fluoxetine around 9.8 and at pH below this value predominate positive species, while above the opposite occurs, the species are neutral near the pH value corresponding to the pKa (Schneider, 2018). Thus, if pH value is between 7.0 and 9.8, there are conditions that enable the sorption process of positively charged compounds, such as fluoxetine, by electrostatic attraction between the fluoxetine (cation) and negatively charge surface (*Chlorella vulgaris*).

For lyophilized microalgae, pH_{PZC} obtained was 5.8 (Figure 6.3), quite close to the value obtained by Heidelmann et al., (2017), for lyophilized *Chlorella vulgaris*, 5.59.

Considering those results and that the pH range allowed for urban wastewater discharge is 6-9, kinetics and equilibriums were performed at pH values between 6 and 8.

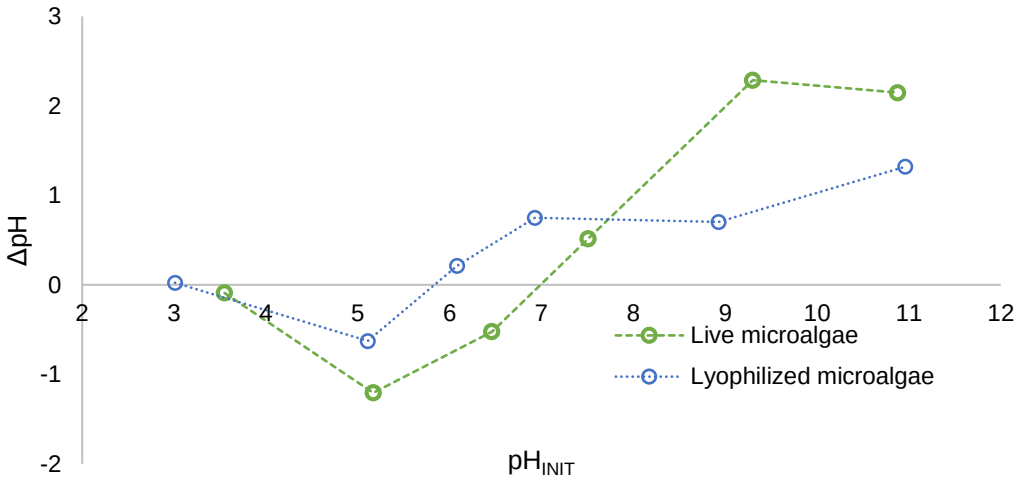

Figure 6.3. Point of zero charge (PZC) determination of live and lyophilized *Chlorella vulgaris*.

6.2.3 Influence of pH

Set aside PZC, the effect of pH in the biosorption of fluoxetine was performed as well. The values of $pH_{INITIAL}$ and pH_{FINAL} (Figure 6.4) were taken for experiments carried out with microalgae and in the absence of it. The blank experimental values both for live and lyophilized microalgae are represented in the same figure. From pH 5 to 7, pH values were practically constant with fluctuations lower than 10 and 5% for live and lyophilized microalgae, respectively. However, it is evident from Figure 6.4 that between pH 7 and 9, the value of pH_{FINAL} is lower than the $pH_{INITIAL}$, and that larger decreases are observed in the experiments without the microalgae. This decrease could indicate possible competition between the formation of hydrated types of fluoxetine and active biosorbent sites or modification of the surface charge of biosorbent (Blázquez et al., 2009).

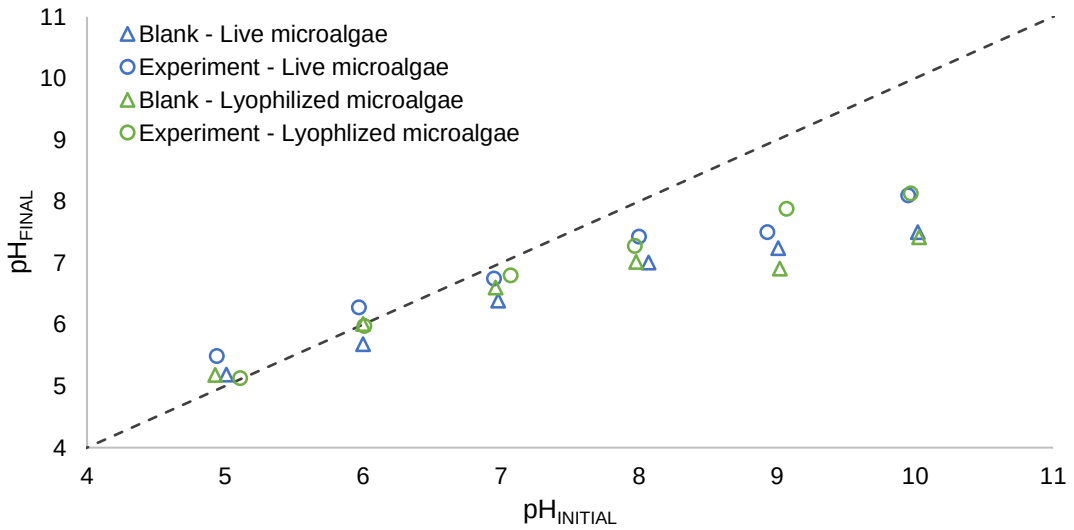

Figure 6.4. pH variation in the blank and experimental (without and with microalgae, respectively) for live and lyophilized microalgae.

Furthermore, the pH_{INITAL} was related to the uptake capacity as can be observed in Figure 6.5, which allowed to identify the most suitable pH for the effective biosorption on *Chlorella vulgaris*. In Figure 6.5, the results show a dependency on the initial pH by changing the biosorption capacity with $pH_{INITIAL}$. As expected, the maximum biosorption capacity is observed at pH 8, which lays in the range 7 (the microalga's pH_{PZC}) to 9.8 (the pKa of fluoxetine hydrochloride) where the electrostatic attraction algae/pharmaceutical is maximum. At pH values below 7, both tend to be positively charged and there is not electrostatic attraction, which explains the decrease of biosorption capacity observed. The slight increase noticed at pH 5 might be related to the significant presence of protons which due to their positive charge may contribute to a protonation of the algae allowing the occurrence of ion exchange.

The data about the effect of pH using lyophilized microalgae was inconclusive and due to lack of time it was not possible to repeat the experiment, however a similar pattern was predictable since there was no change in the functional groups of the microalgae after lyophilization.

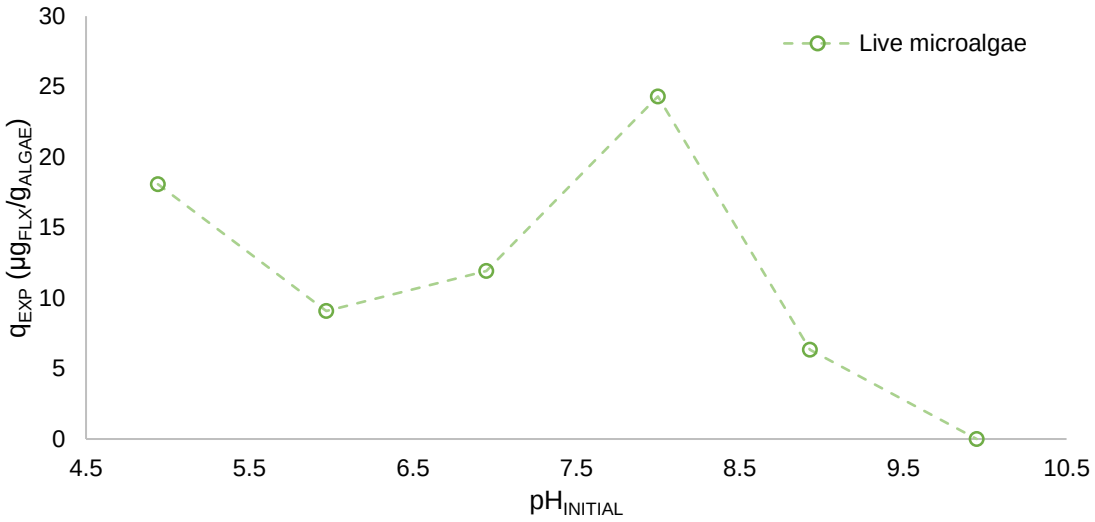

Figure 6.5. Influence of pH on the biosorption capacity of fluoxetine.

6.3 Kinetic studies

Kinetic studies were performed to find the required time that the system would take to achieve the equilibrium and the sorption capacity for each sample at 25ºC, in the pH range 7.3-7.7. Since these pH values were included in the range of higher adsorption capacity of live microalgae (Figure 6.5), pH was not adjusted. The experimental uptake rates of fluoxetine by live and lyophilized microalgae were studied without pH adjustment for an initial fluoxetine concentration around 450 and 600 $\mu g_{FLX}/L$ and an adsorbent dose of 0.126 and 0.138 g_{ALGAE}/L, respectively. The experimental results were applied to three empirical adsorption models and two diffusional models: pseudo-first order, pseudo-second order, Elovich, external mass diffusion and intraparticle diffusion models in order to analyse the rate of adsorption and the mechanisms involved in the adsorption of fluoxetine onto microalgae.

The adsorption by live *Chlorella vulgaris* was quite fast within the first 15 min of the experiment as can be seen in Figure 6.6, around 24% of the fluoxetine was removed. Equilibrium was reached after 20 min corresponding to 26.6% removal and experimental maximum fluoxetine absorbed per amount of adsorbent of 967.9 $\mu g_{FLX}/g_{ALGAE}$. During the assay (2 h), there was a slight increase (lower than 5%) on the biomass concentration, which was considered insignificant. The initial rapid phase may correspond to adsorption or ion exchange on the cell surface. After the initial phase, there was not a significant difference in the adsorption capacity, which may be attributed to the saturation of binding sites. Other mechanisms, such as bioaccumulation biodegradation, biomineralization, volatilization and photodegradation, were assumed that did not occur since the conditions of operation and the short contact time (2 h) would not favour their occurrence, and in the case of volatilization Henry's Law constant of fluoxetine is low (2.46×10^{-5}) (AMAP Chemicals, 2019).

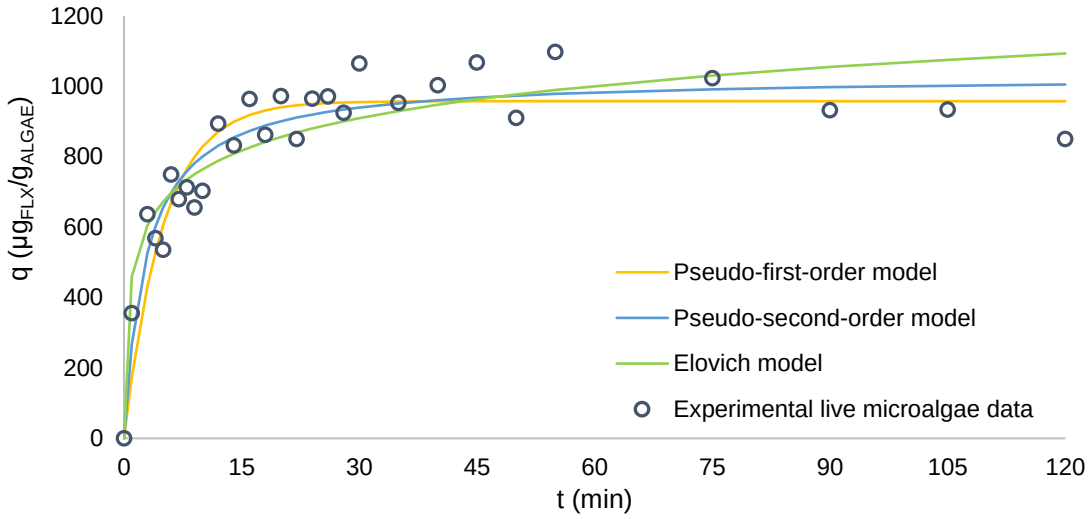

Figure 6.6. Experimental kinetics adsorption data and pseudo-first order, pseudo-second order and Elovich models related to living microalgae.

The sorption by lyophilized microalgae was faster than live microalgae as can be seen in Figure 6.7, 49% of the fluoxetine was removed within the first 10 min followed by a fast approach to equilibrium (around 55% of removal efficiency). In the equilibrium, the experimental capacity of *Chlorella vulgaris* was 2487.7 $\mu g_{FLX}/g_{ALGAE}$ that was achieved 15 min after the first contact.

Since biosorption is a fast process consisting only in physic-chemical sorption and ion exchange in microalgae cell walls, it would be expected that equilibrium would be reached quickly, and through the results, from the experiments with live and dead microalgae, it was possible to confirm it. Since adsorption (physico-chemical) is the main mechanism involved and being this independent of algal metabolism, similar results were expected between dead and live microalgae. Functional groups such as amines, carboxyl, sulphates, phosphates and imidazoles present in the polysaccharides and proteins offer possible binding sites in the cell walls for drugs such as fluoxetine. These allow algae to generally exhibit a negative charge, being favourable for attracting positive charges, such as the one of fluoxetine when the pH is below 9.8 (Tam et al.,

2002). Although the difference of the time required for algae to reach equilibrium was relatively minimal, adsorption by the dead cells occurred almost instantaneously when the algae contacted the fluoxetine solution. Experimentally, the removal of fluoxetine by dead *Chlorella vulgaris* was twice higher than the rate of removal by living microalgae, which means that a change in the cells may have occurred during the lyophilization process. As previously mentioned, lyophilization can lead to lysis of the cells, which will allow the biosorption by the membranes of organelles and other intracellular members exposed to fluoxetine and thus explain the difference in biosorption capacities (Tam et al., 2002). In addition to, according to Serra (2015), due to the lyophilization process, there is an increase of porosity of the wall and an increase of the average pore diameter (Cavalvante, 2003), thereafter, the surface area of contact with the solution will increase and the biosorption capacity of the dead algae as well.

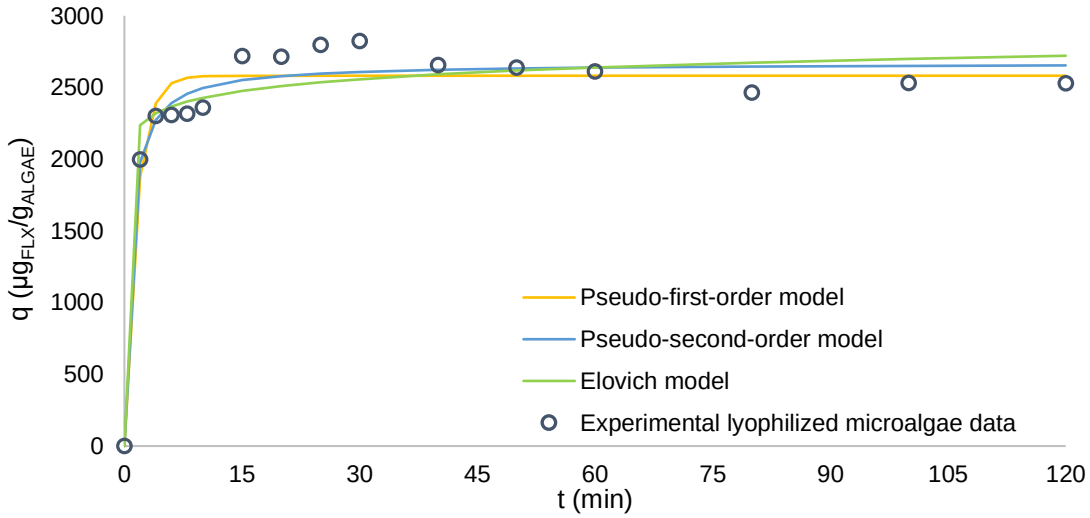

Figure 6.7. Experimental kinetics adsorption data and pseudo-first order, pseudo-second order and Elovich models related to lyophilized microalgae.

The values of the kinetic parameters obtained by the modelling through empirical kinetic models and the respective statistical analysis are presented in Table 6.2.

The best fit model was the pseudo-second order model, which is the one with the lowest SSE value and the higher R^2_{adj} which the values obtained by the model were closer to the experimental values and had a better correlation. The error increased in the following order: pseudo-second order < pseudo-first order < Elovich, both for living and dead algae. Beyond the SSE and R^2_{adj}, the pseudo-second order model was the one which presented the lower X^2_{red}, AIC and BIC also. To reinforce these results, according to the F-test, all other models showed a F_{calc} lower than critical F, hence models such as pseudo-first order and Elovich did not show evidence of being more adequate to define the experimental data than pseudo-second order model. Thus, according to the results, pseudo-second order model could be put forward for the adsorption of fluoxetine by live and dead microalgae. The pseudo-second order model assumes that adsorption occurs at specific sites and there is no interaction between adsorbed molecules; the adsorption energy is independent on the surface coverage; the maximum adsorption capacity corresponding

to the saturation of adsorbate on the monolayer of the surface of the adsorbent and the adsorbate concentration is constant.

Therefore, fluoxetine was adsorbed at a higher rate (K_2) by the dead than living microalgae, $5.4\times10^{-4}\pm1.3\times10^{-4}$ and $3.4\times10^{-4}\pm1.3\times10^{-4}$ $g_{ALGAE}/(\mu g_{FLX}.min)$, respectively. This faster access to active sites is probably related to physical changes caused by lyophilization. Comparing the adsorption capacities achieved at equilibrium ($q_{CAL,EQ}$), live microalgae got a higher value, 1029±58 $\mu g_{FLX}/g_{ALGAE}$ than dead *Chlorella vulgaris*, 2670±47 $\mu g_{FLX}/g_{ALGAE}$, but conclusions related with this subject can only be made after studying the whole range of concentration in equilibrium studies.

Table 6.2. Kinetic parameters of reaction models for the adsorption of fluoxetine onto *Chlorella vulgaris*.

Model	Parameters	Live Microalgae	Lyophilized Microalgae
Pseudo-first order	K_1 (1/min)	0.20±0.05	0.6±0.1
	$q_{CAL,\ EQ}$ ($\mu g_{FLX}/g_{ALGAE}$)	957±47	2582±45
	SSE	217208	351099
	$S_{y.x}$	89.7	158.4
	X^2_{red}	8045	25078
	R^2_{adj}	0.857	0.944
	A.I.C.	262.7	163.9
	B.I.C.	265.5	165.48
	F_{calc}	0.798	0.693
	$F_{0.05;27;27}$	1.905	2.483
Pseudo-second order	K_2 ($g_{ALGAE}/(\mu g_{FLX}.min)$)	$3.4\times10^{-4}\pm1.3\times10^{-4}$	$5.4\times10^{-4}\pm1.3\times10^{-4}$
	$q_{CAL,EQ}$ ($\mu g_{FLX}/g_{ALGAE}$)	1029±58	2670±47
	SSE	173419	243299
	$S_{y.x}$	80.1	131.8
	X^2_{red}	6423	17379
	R^2_{adj}	0.886	0.961
	A.I.C.	256.2	158.1
	B.I.C.	258.9	159.6
	F_{calc}	1.000	1.000
	$F_{0.05;27;27}$	1.905	2.483
Elovich model	α_E ($\mu g_{FLX}/(g_{ALGAE}\cdot min)$)	$4.2\times10^{3}\pm6.0\times10^{3}$	$1.0\times10^{10}\pm6.6\times10^{10}$
	β_E ($g_{ALGAE}/\mu g_{FLX}$))	$7.6\times10^{-3}\pm1.9\times10^{-3}$	$8.5\times10^{-3}\pm2.7\times10^{-3}$
	SSE	261040	428133
	$S_{y.x}$	98.3	174.9
	X^2_{red}	18633	30581
	R^2_{adj}	0.828	0.931
	A.I.C.	268.0	167.1
	B.I.C.	270.8	168.7
	F_{calc}	0.664	0.568
	$F_{0.05;27;27}$	1.905	2.483

The results were also adjusted to the diffusion models (intraparticular and external). The fits of the intraparticular diffusion model for to the experimental results obtained for live and dead microalgae are shown in Figure 6.8 and Figure 6.9, respectively.

By observing both graphs, it was clear that intraparticular diffusion was not the only process that could limit the withdrawal of fluoxetine since there is more than one section with a linear tendency. Both for living and dead algae, there are three linear sections. The first linear section represented fluoxetine migration from the bulk of the solution of the boundary film surrounding to the adsorbent surface, followed by the second section in which intraparticular diffusion was the limiting step and a third section, where adsorption equilibrium was reached. Since the results did not cross the origin, the intraparticular diffusion was not considered the only process limiting the adsorption. The intraparticular diffusion constant could be determined by the slope of the second linear section. The largest intraparticular diffusion rate (K_{ID}) was reached by dead algae (112±47 $\mu g_{FLX}/(g_{ALGAE} \cdot min^{1/2})$), while by living algae, the K_{ID} was 61±4 $\mu g_{FLX}/(g_{ALGAE} \cdot min^{1/2})$, due to the greater porosity of the microalgae cell walls obtained after lyophilization. The interception of the second section with the Y-axis provided information regarding the thickness of the boundary layer (C_{ID}). Lyophilized algae showed higher C_{ID} than the live algae suggesting that in the dead algae the superficial diffusion was a more important mass transfer resistance than for live algae. However, the linear tendencies did not display a strong correlation ($R^2 > 0.99$), which showed that this model did not have the most coherent adjustment to the system, so intraparticular diffusion was not the limiting mass transfer resistance. The adjusted correlation coefficients of the second section, for live and dead microalgae, were 0.34 and 0.84, respectively.

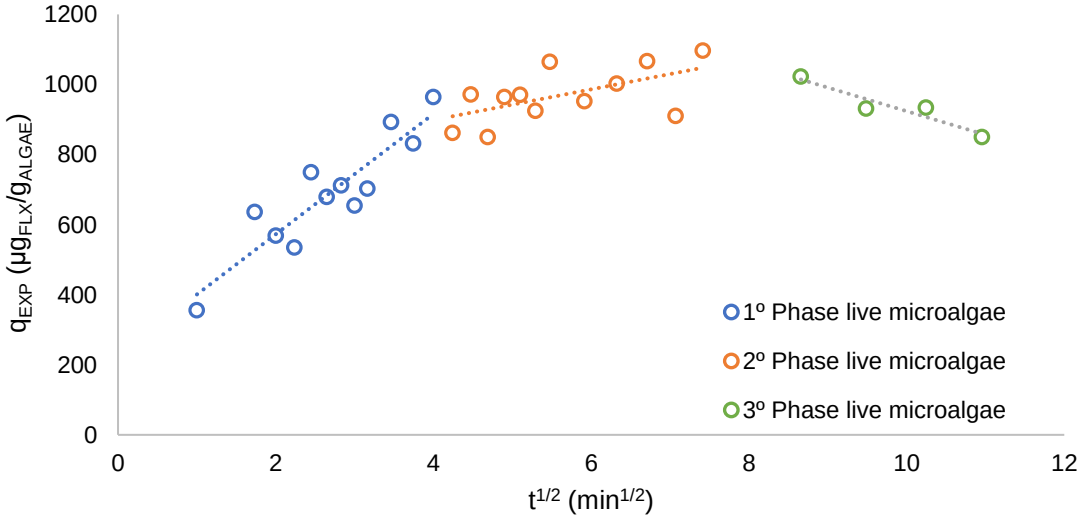

Figure 6.8. Intraparticular diffusion linear model related to live microalgae.

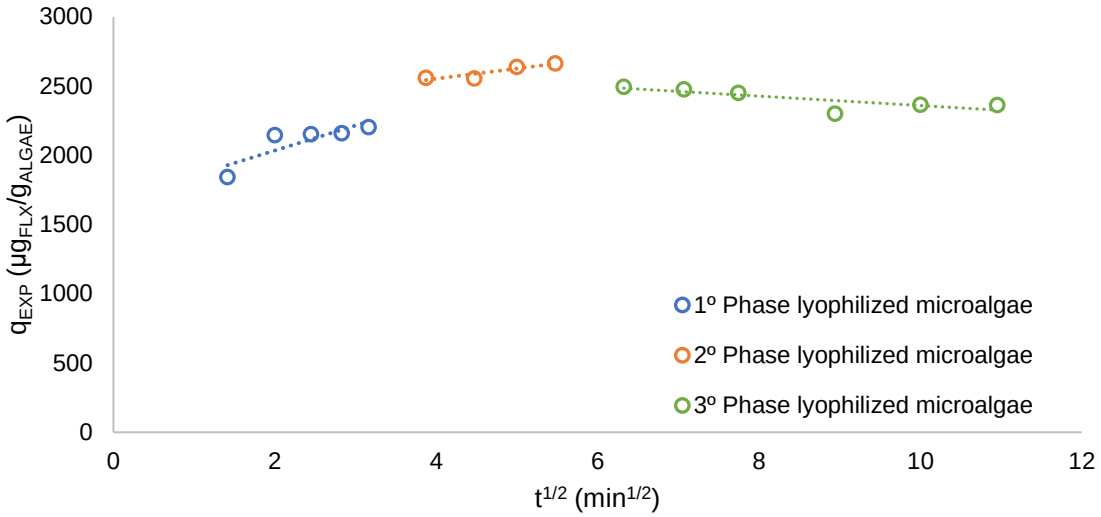

Figure 6.9. Intraparticular diffusion linear model related to lyophilized microalgae.

In Figure 6.10 is shown the experimental data adjusted to the external diffusion model for live and lyophilized microalgae. This model was applied to the results obtained at the beginning of the experiment. The correlations for live algae and lyophilized algae were weak, 0.75 and 0.61, respectively. Thus, this model was excluded to represent the process of adsorption of fluoxetine. This was a confirmation of the mentioned in Section 4.1.5, since during the procedure, constant stirring was applied, reducing the external film and consequently reducing this resistance to mass transfer.

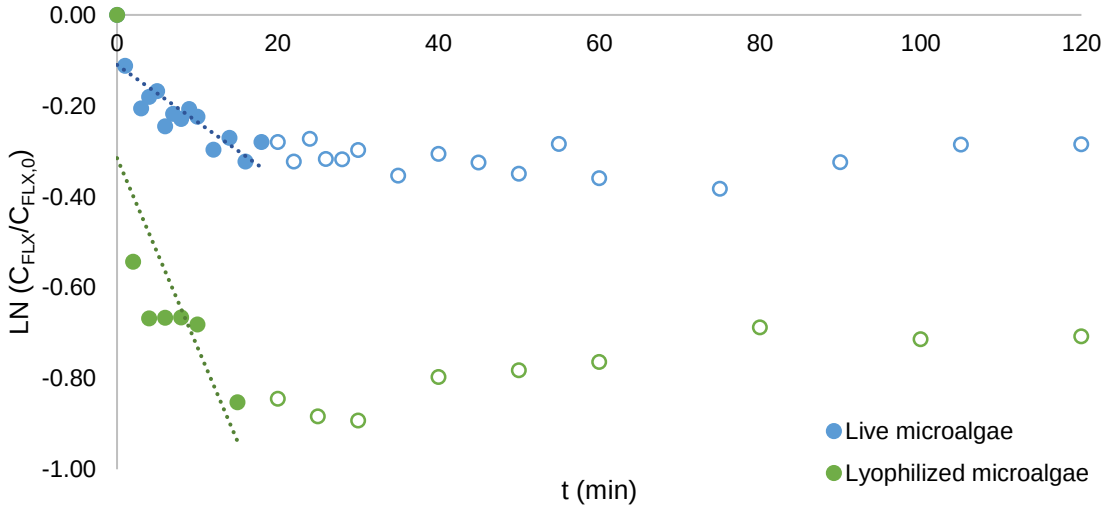

Figure 6.10. External mass diffusion model related to live and lyophilized microalgae.

6.4 Equilibrium studies

Equilibrium studies were performed for 2 h in order to guarantee that the equilibrium was reached. There are several mathematical models that can describe adsorption phenomena. In this study, six models were selected to fit the experimental data: Langmuir, Freundlich, Sips,

Redlich-Peterson, Tóth and Flory-Huggins models. Their respective parameters and corresponding statistical parameters are presented in Table 6.3.

Table 6.3. Parameters of equilibrium models for the adsorption of fluoxetine onto Chlorella vulgaris.

Model	Parameters	Live Microalgae	Lyophilized Microalgae
Langmuir's model	K_L (L/μg_{FLX})	$2.0\times10^{-2}\pm0.5\times10^{-2}$	$1.1\times10^{-2}\pm0.3\times10^{-2}$
	$q_{MAX,L}$ ($\mu g_{FLX}/g_{ALGAE}$)	$1.9\times10^{3}\pm0.1\times10^{3}$	$1.6\times10^{3}\pm0.2\times10^{3}$
	SSE	176337	43004
	$S_{y.x}$	133	73
	X^2_{red}	17634	5375
	R^2_{adj}	0.940	0.975
	A.I.C.	119.1	87.7
	B.I.C.	120.1	88.3
	F_{calc}	1.000	1.000
	$F_{0.05;\ d.f.1;\ d.f.2}$	2.980	3.440
Freundlich's model	K_F (L/g_{ALGAE})	205±49	66±21
	n_F	2.7±0.3	1.8±0.2
	SSE	231193	66038
	$S_{y.x}$	152	91
	X^2_{red}	23119	8255
	R^2_{adj}	0.922	0.961
	A.I.C.	122.4	92.0
	B.I.C.	123.4	92.6
	F	0.763	0.651
	$F_{0.05;\ d.f.1;\ d.f.2}$	2.980	3.440
Sips' model	q_{MS} ($\mu g_{FLX}/g_{ALGAE}$)	$2.1\times10^{3}\pm0.5\times10^{3}$	$1.5\times10^{3}\pm0.4\times10^{3}$
	K_S (L/μg_{FLX})	0.03±0.02	$1.0\times10^{-2}\pm0.8\times10^{-2}$
	MS	0.9±0.3	1.1±0.3
	$S_{y.x}$	171523	42700
	SYX	138	78
	X^2_{red}	19058	6100
	R^2_{adj}	0.936	0.971
	A.I.C.	120.8	89.6
	B.I.C.	122.3	90.5
	F	0.925	0.881
	$F_{0.05;\ d.f.1;\ d.f.2}$	2.980	3.440
Redlich-Peterson's model	K_{RP} (L/g_{ALGAE})	52±30	20±10
	a_{RP} (L/μg_{FLX})	0.06±0.09	0.02±0.05
	β_{RP}	0.9±0.2	0.9±0.4
	SSE	164447	42510
	$S_{y.x}$	135	78
	X^2_{red}	18272	6073
	R^2_{adj}	0.938	0.971
	A.I.C.	120.3	89.5

	B.I.C.	121.8	90.5
	F	0.965	0.885
	$F_{0.05;\ d.f.1;\ d.f.2}$	2.980	3.440
Tóth's model	K_T (L/μg_{FLX})	0.03±0.01	$1.1\times10^{-2}\pm0.3\times10^{-2}$
	$q_{MAX,T}$ ($\mu g_{FLX}/g_{ALGAE}$)	$2.3\times10^{3}\pm0.9\times10^{3}$	$1.7\times10^{3}\pm1.0\times10^{3}$
	n_T	0.7±0.5	0.9±0.7
	SSE	168524	42894
	$S_{y.x}$	137	78
	X^2_{red}	18725	6128
	R^2_{adj}	0.937	0.971
	A.I.C.	120.6	89.6
	B.I.C.	122.1	90.5
	F	0.942	0.877
	$F_{0.05;\ d.f.1;\ d.f.2}$	2.980	3.440
Flory-Huggins' model	n_{FH}	0.5±0.2	0.6±0.1
	K_{FH} (L/μg_{FLX})	1039±1	1160±1
	R^2_{adj}	0.315	0.510

For live and dead microalgae, the selected models had reasonable adjustments except for Freundlich and Flory-Huggy isotherm models, since they showed a low R^2_{adj} value and the Freundlich model also had a high SSE among all models. A poor fit of the Freundlich mathematical model could be observed and a low correlation between experimental and adjusted values of the Flory-Huggins linear model in Figure 6.11 to Figure 6.13.

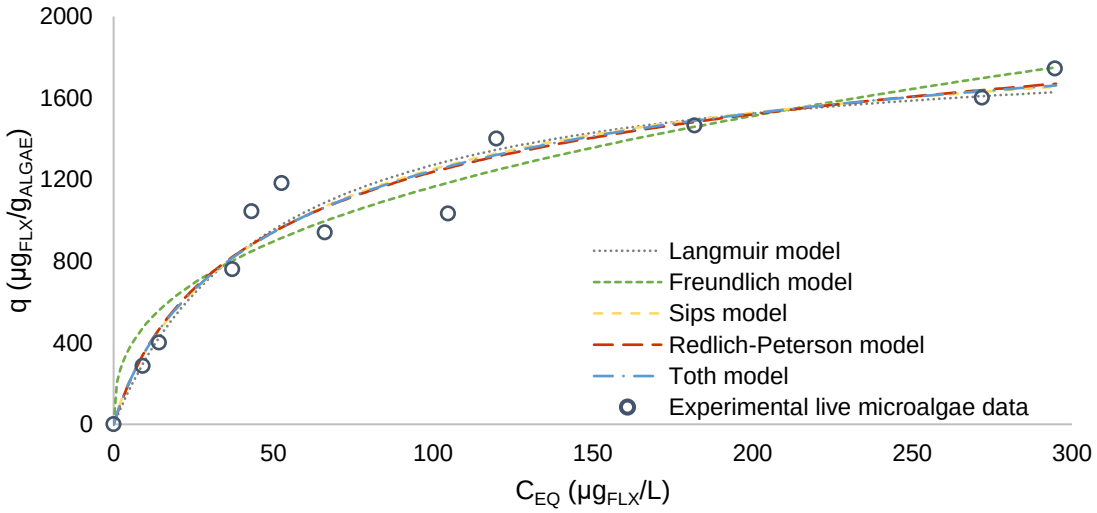

Figure 6.11. Experimental equilibrium adsorption data and Langmuir, Freundlich, Sips, Redlich-Peterson and Tóth models related to live microalgae.

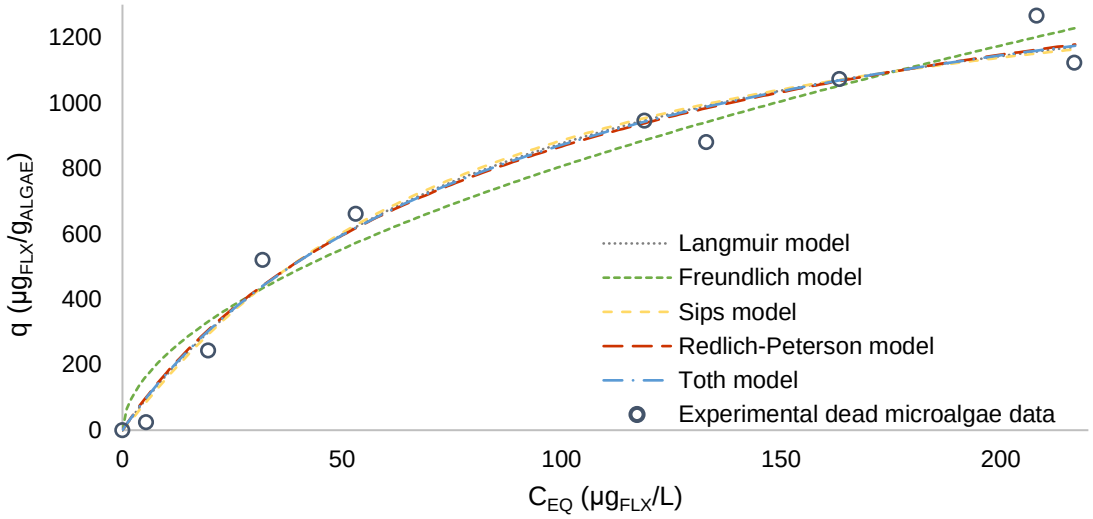

Figure 6.12. Experimental equilibrium adsorption data and Langmuir, Freundlich, Sips, Redlich-Peterson and Tóth models related to lyophilized microalgae.

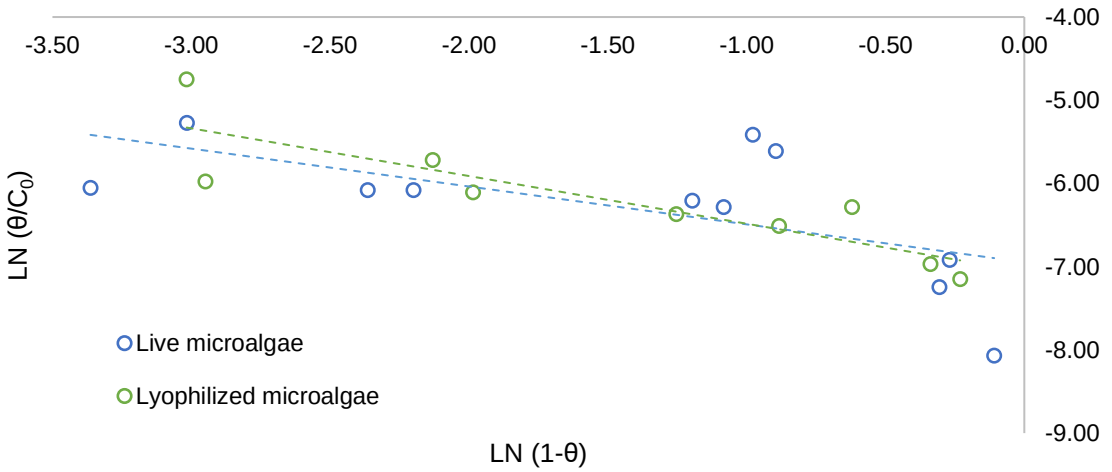

Figure 6.13. Flory-Huggins linear model related to live and lyophilized microalgae.

The error increases in the following order: Langmuir <Redlich <Tóth <Sips. In relation to Redlich model, although this model presented the lowest SSE, it was not the one with the lowest $S_{y.x}$, X^2_{red}, AIC and BIC and the highest correlation (R^2_{adj}) and furthermore, the errors associated with the parameters were high in relation to their values.

Between, Langmuir, Sips and Tóth models, there was a significant difference in the statistical error parameters but both for live and dead microalgae, equilibrium results were better described by the Langmuir model which was the one with higher R^2_{adj}, lower X^2_{red}, AIC and BIC which means that it is suitable to this system and there was a smaller loss of information when the experimental data are represented by the adjusted model. In addition, the Langmuir model is one of the simplest models to describe an adsorption phenomenon. Test-F was applied and

considering Langmuir as the reference model, all models presented a lower F_{calc} than critical F value, which reinforces the choice of the Langmuir model.

Thus, Langmuir model describes the process of fluoxetine adsorption by microalgae and is valid for monolayer sorption onto a surface that is homogeneously distributed by identical sites over the sorbent surface, this is also in accordance with the hypothesis assumed by the pseudo-second order kinetic model. The maximum capacity ($q_{MAX,L}$) for living algae was 1.9±0.1 mg_{FLX}/g_{ALGAE}, slightly higher than for dead microalgae which were 1.6±0.2 mg_{FLX}/g_{ALGAE}. Considering the results of the kinetic studies, the capacities for lyophilized microalgae were expected to be higher than for live microalgae since changes in the structure of the microalgae cell walls that may have occurred during lyophilization would contribute to higher porosity and consequently a higher biosorption capacity. Thus, the surface area after lyophilization should be determined, to verify if lyophilization actually increased the area of contact between fluoxetine and the algal surface area. The kinetic and equilibrium results suggest that lyophilization had an effect on the physical characteristics of algae providing a more accessible structure that has favoured the kinetics of adsorption, however this did not cause an increase in the adsorption capacity. The higher adsorption capacity observed in live algae might be related to other phenomena besides adsorption that are responsible for fluoxetine removal, namely metabolic processes that only occur when the algae is alive, such as biodegradation and biomineralization.

Despite that, q_{MAX} gives important information, useful to predict the adsorbent performance in real systems and to design adsorbers at different scales. In wastewater treatment, the adsorbent materials that have a longer useful lifetime, are the ones with higher q_{MAX} values (Coimbra et al., 2018). From the follow-up of the results, the Langmuir constant (K_L), that is related to the affinity of the binding sites, was $2.0\times10^{-2}\pm0.5\times10^{-2}$ $L/\mu g_{FLX}$ for live algae, which is about twice the constant of the dead algae, $1.1\times10^{-2}\pm0.3\times10^{-2}$ $L/\mu g_{FLX}$, however these values show the same level of magnitude.

The shape of the Langmuir isotherm also gives information on whether the sorption process is favourable or unfavourable in a batch sorption process. The dimensionless separation factor (R_L) was 0.14 and 0.22 for live and dead *Chlorella vulgaris*, respectively. Being this value between 0 and 1 indicates that the process is favourable.

The maximum monolayer adsorption capacity was compared, under identical experimental conditions, with other adsorbent capacities reported in the literature, as it can be seen in Table 6. 4. In general, the q_{MAX} of *Chlorella vulgaris* was quite low comparing among all biomasses, mainly with paper mill sludge and carbon activated. Although the adsorption capacity of *Chlorella vulgaris* was only comparable with the hollow tree and vine *Chlorella vulgaris* is still a promissory adsorbent to uptake fluoxetine and a deeper investigation should be done in order to optimize the process.

Table 6. 4. Comparison of biosorption capacity for fluoxetine with several adsorbents.

Adsorbent	**Conditions**		**q_{MAX}**	**References**
	Time (h)	**T (ºC)**	**(mg_{FLX}/g)**	
Commercial activated carbon	<6	25	96.2	(Jaria et al., 2015)
Paper mill sludge-based nonactivated carbon	<6	25	120.4	
Paper mill sludge-based activated carbon with $ZnCl_2$	<6	25	28.4	
Paper mill sludge-based activated carbon with NaOH	<6	25	136.6	
Eucalyptus	0.25	~20	6.41	(Fernandes et al., 2019)
Hollow tree	0.25	~20	3.04	
Vine	0.25	~20	2.80	
Bifurcaria bifurcata macroalgae	3	~20	6.81	(Silva et al., 2019)
Live/dead *Chlorella vulgaris* microalgae	2	~20	1.90/ 1.64	Current study

7. Conclusions and future suggestions

Biosorption onto microalgae was investigated in order to remove the pharmaceutical fluoxetine, an environmental emerging pollutant, often found in the environment.

The microalga *Chlorella vulgaris* was chosen as biosorbent because of its characteristics, non-toxic, easily cultured and a fast growth species. Moreover, it has already shown promising results in this field.

Its performance in the living and dead state (after lyophilization) was studied. The removal of fluoxetine by algae may be due to different mechanisms, such as biosorption, bioaccumulation and metabolic processes, therefore, it may be expected some differences in behaviour between them.

A characterization of live and lyophilized algae was performed concerning FTIR analysis and determination of pH_{PZC}. Since biosorption is a process that is affected by pH, its influence was also studied in the range 5 to 10. Kinetic and equilibrium studies were performed, the results were analysed, and different models were fitted to them.

FTIR analysis allowed to identify the functional groups such as hydroxyl, sulfonic and carboxylic, that may play the main role in the biosorption process. The pH at the point of zero charge was 7.0 and 5.8 for living and dead microalgae, respectively. The dependency of pH was observed in relation to living microalgae. The most favourable pH values for biosorption were found in the range between 7.0 (live algae's pH_{PZC}) and 9.8 (adsorbate's pKa), where electrostatic attraction between microalgae (negatively charged) and fluoxetine (positively charged) was maximum. The effect of pH using lyophilized microalgae was inconclusive suggesting that it should be repeated prior to take conclusions.

The best-fitting kinetic model was the pseudo-second order, for both for live and lyophilized algae. Furthermore, the time required to achieve equilibrium, was very similar, 15 and 20 min respectively for lyophilized and live algae. Lyophilization process may be responsible for the faster removal of fluoxetine since it may increase the permeability of microalgae cell walls, allowing faster access to biosorption sites.

Regarding the equilibrium experimental results, the Langmuir model (favourable isothermal) showed to be the one with the best fit. The maximum adsorption capacities according to the Langmuir model were $1.9\times10^3\pm0.1\times10^3$ and $1.6\times10^3\pm0.2\times10^3$ $\mu g_{FLX}/g_{ALGAE}$ for live and lyophilized algae, respectively. The higher uptake capacity was expected in dead microalgae since lyophilization could have introduced physical changes (pores in cell walls) that would increase both accessibility and specific surface area. However live microalgae showed higher biosorption capacity than dead, which may be attributed to fluoxetine removal by other phenomena besides biosorption, namely metabolic processes. In addition to the maximum capacity, the Langmuir model gave information on the affinity of the binding sites. Live algae had a higher affinity to the binding sites (0.020 ± 0.005 L/μg_{FLX}), thus a higher adsorption capacity, than the dead algae, which presented almost half of the affinity (0.011 ± 0.003 L/μg_{FLX}), corresponding also to lower adsorption capacities Even with a better removal obtained for living microalgae cells,

dead *Chlorella vulgaris* could be advantageous for removal of fluoxetine from contaminated wastewater, since it does require less maintenance and, furthermore, as its metabolism is deactivated, it is not affected by the presence of toxicants.

Comparing with some results with other adsorbents from literature, *Chlorella vulgaris* showed a low adsorbent capacity. However, it is still a promissory adsorbent to uptake fluoxetine as an alternative tertiary treatment in wastewater.

Some suggestions for future works are provided below considering the results obtained.

It was suggested to repeat the study of the pH influence prior to make conclusions.

A determination of the surface area of lyophilized *Chlorella vulgaris* would be required to verify if lyophilization really increases the surface area.

Research on fixed-bed column tests should be performed at the laboratory scale and optimization of operational parameters in order to allow their application, posteriorly, at industrial level.

Other microalgae performances should be evaluated, namely the removal of other emerging pollutants that are found in the environment.

Experiments with real wastewater contaminated with fluoxetine should be the next step.

The research of ways for valorising this biomass after use should be found.

References

Abdel-Raouf, N., Al-Homaidan, A.A., Ibraheem, I.B.M., 2012. Microalgae and wastewater treatment. Saudi J. Biol. Sci. 19, 257–275. https://doi.org/10.1016/J.SJBS.2012.04.005

Aksu, Z., 2002. Determination of the equilibrium, kinetic and thermodynamic parameters of the batch biosorption of nickel(II) ions onto Chlorella vulgaris. Process Biochem. 38, 89–99. https://doi.org/10.1016/S0032-9592(02)00051-1

Al-Muhtaseb, A.H., Ibrahim, K.A., Albadarin, A.B., Ali-khashman, O., Walker, G.M., Ahmad, M.N., 2011. Remediation of phenol-contaminated water by adsorption using poly(methyl methacrylate) (PMMA). Chem. Eng. J. 168, 691–699. https://doi.org/10.1016/j.cej.2011.01.057

AMAP Chemicals, 2019. Fluoxetine [WWW Document]. URL https://chemicals.amap.no/chemicals/fluoxetine/ (accessed 10.1.19).

Andrès, Y., Thouand, G., Boualam, M., Mergeay, M., 2000. Factors influencing the biosorption of gadolinium by micro-organisms and its mobilisation from sand. Appl. Microbiol. Biotechnol. 54, 262–267. https://doi.org/10.1007/s002530000368

Archangel'skij, I. V., 2013. Non-Isothermal Kinetic Methods. Ed. Open Access.

Barbosa, M.O., Moreira, N.F.F., Ribeiro, A.R., Pereira, M.F.R., Silva, A.M.T., 2016. Occurrence and removal of organic micropollutants: An overview of the watch list of EU Decision 2015/495. Water Res. 94, 257–279. https://doi.org/10.1016/J.WATRES.2016.02.047

Bilal, M., Rasheed, T., Eduardo Sosa-Hernández, J., Raza, A., Nabeel, F., N Iqbal, H.M., 2018. Biosorption: an interplay between marine algae and potentially toxic elements-A review. Mar. Drugs 16. https://doi.org/10.3390/md16020065

Blázquez, G., Hernáinz, F., Calero, M., Martín-Lara, M.A., Tenorio, G., 2009. The effect of pH on the biosorption of Cr (III) and Cr (VI) with olive stone. Chem. Eng. J. 148, 473–479. https://doi.org/10.1016/J.CEJ.2008.09.026

Bodin, H., Daneshvar, A., Gros, M., Hultberg, M., 2016. Effects of biopellets composed of microalgae and fungi on pharmaceuticals present at environmentally relevant levels in water. Ecol. Eng. 91, 169–172. https://doi.org/10.1016/J.ECOLENG.2016.02.007

Borao, R.A., 2015. Oxidation of pharmaceuticals by chlorine dioxide in wastewater effluents. Royal Institute of Technology.

Bu, Q., Shi, X., Yu, G., Huang, J., Wang, B., 2016. Assessing the persistence of pharmaceuticals in the aquatic environment: challenges and needs. Emerg. Contam. 2, 145–147. https://doi.org/10.1016/j.emcon.2016.05.003

Cavalvante, J., 2003. Análise experimental da cinética de secagem da alga marinha Sargassum sp. Universidade Estadual de Campinas.

Chen, C.-L., Chang, J.-S., Lee, D.-J., 2015. Dewatering and Drying Methods for Microalgae. Dry. Technol. 33, 443–454. https://doi.org/10.1080/07373937.2014.997881

Chen, Z., Ma, W., Han, M., 2008. Biosorption of nickel and copper onto treated alga (Undaria pinnatifida): Application of isotherm and kinetic models. J. Hazard. Mater. 155, 327–333.

https://doi.org/10.1016/j.jhazmat.2007.11.064

Cho, D., Lee, S., Park, S., Chung, A., 1994. Studies on the biosorption of heavy metals onto Chlorella vulgaris. J. Environ. Sci. Heal. . Part A Environ. Sci. Eng. Toxicol. 29, 389–409. https://doi.org/10.1080/10934529409376043

Coimbra, R., Escapa, C., Vázquez, N., Noriega-Hevia, G., Otero, M., Coimbra, R.N., Escapa, C., Vázquez, N.C., Noriega-Hevia, G., Otero, M., 2018. Utilization of Non-Living Microalgae Biomass from Two Different Strains for the Adsorptive Removal of Diclofenac from Water. Water 10, 1401. https://doi.org/10.3390/w10101401

Crini, G., Lichtfouse, E., 2018. Green adsorbents for pollutant removal : fundamentals and design. Springer.

Crist, R.H., Oberholser, K., Shank, N., Ming Nguyen, ., 1981. Nature of bonding between metallic ions and algal cell walls. Environ. Sci. Technol. 15, 1212–1217. https://doi.org/10.1021/es00092a010

Cuellar-Bermudez, S.P., Aleman-Nava, G.S., Chandra, R., Garcia-Perez, J.S., Contreras-Angulo, J.R., Markou, G., Muylaert, K., Rittmann, B.E., Parra-Saldivar, R., 2017. Nutrients utilization and contaminants removal. A review of two approaches of algae and cyanobacteria in wastewater. Algal Res. 24, 438–449. https://doi.org/10.1016/J.ALGAL.2016.08.018

Doerr-MacEwen, N.A., 2007. The management of human pharamaceiticals in the environemnt. University of Waterloo.

Driver, T., Bajhaiya, A.K., Allwood, J.W., Goodacre, R., Pittman, J.K., Dean, A.P., 2015. Metabolic responses of eukaryotic microalgae to environmental stress limit the ability of FT-IR spectroscopy for species identification. Algal Res. 11, 148–155. https://doi.org/10.1016/J.ALGAL.2015.06.009

DrugBank, 2019. Fluoxetine hydrochloride [WWW Document]. URL https://www.drugbank.ca/salts/DBSALT000087 (accessed 9.29.19).

El-Bassat, R., Touliabah, H., Harisa, G., 2012. Toxicity of four pharmaceuticals from different classes to isolated plankton species. African J. Aquat. Sci. 37, 71–80. https://doi.org/10.2989/16085914.2012.666376

Escapa, C., Coimbra, R.N., Paniagua, S., García, A.I., Otero, M., 2015. Nutrients and pharmaceuticals removal from wastewater by culture and harvesting of Chlorella sorokiniana. Bioresour. Technol. 185, 276–284. https://doi.org/10.1016/J.BIORTECH.2015.03.004

European Parliament, 2013. Directive 2013/39/EU of the European Parliament and of the Council. Off. J. Eur. Union.

Fernandes, M.J., Moreira, M.M., Paíga, P., Dias, D., Bernardo, M., Carvalho, M., Lapa, N., Fonseca, I., Morais, S., Figueiredo, S., Delerue-Matos, C., 2019. Evaluation of the adsorption potential of biochars prepared from forest and agri-food wastes for the removal of fluoxetine. Bioresour. Technol. 121973. https://doi.org/10.1016/J.BIORTECH.2019.121973

Florey, K., 1990. Analytical profiles of drug substances - Volume 19. Academic Press.

Flory, P.J., 1953. Principles of Polymer Chemistry. Ithaca, N.Y. : Cornell University Press.

Freundlich, H.M.F., 1906. Over the adsorption in solution. J. Phys. Chem. 57, 385–471.

Furusawa, T., Smith, J.M., 1973. Fluid-Particle and Intraparticle Mass Transport Rates in Slurries. Ind. Eng. Chem. Fundam. 12, 197–203. https://doi.org/10.1021/i160046a009

Griffiths, M.J., Garcin, C., Van Hille, R.P., Harrison, S.T.L., 2011. Interference by pigment in the estimation of microalgal biomass concentration by optical density. J. Microbiol. Methods 85, 119–123. https://doi.org/10.1016/j.mimet.2011.02.005

Guldhe, A., Kumari, S., Ramanna, L., Ramsundar, P., Singh, P., Rawat, I., Bux, F., 2017. Prospects, recent advancements and challenges of different wastewater streams for microalgal cultivation. J. Environ. Manage. 203, 299–315. https://doi.org/10.1016/j.jenvman.2017.08.012

Hadjoudja, S., Deluchat, V., Baudu, M., 2010. Cell surface characterisation of Microcystis aeruginosa and Chlorella vulgaris. J. Colloid Interface Sci. 342, 293–299. https://doi.org/10.1016/j.jcis.2009.10.078

Heidelmann, G.P.., Roldão, T.M.., Egler, S.G.., Nascimento, M.., Giese, E.C., 2017. Uso de biomassa de microalga para biossorção de lantanídeos. Rio de Janeiro. https://doi.org/10.15628/holos.2017.6436

Held, P., 2011. Monitoring of algal growth using their intrinsic properties use of a multi-mode monochromator-based microplate.

Ho, Y.S., McKay, G., 1999. Pseudo-second order model for sorption processes. Process Biochem. 34, 451.

Hom-Diaz, A., Jaén-Gil, A., Bello-Laserna, I., Rodríguez-Mozaz, S., Vicent, T., Barceló, D., Blánquez, P., 2017. Performance of a microalgal photobioreactor treating toilet wastewater: Pharmaceutically active compound removal and biomass harvesting. Sci. Total Environ. 592, 1–11. https://doi.org/10.1016/J.SCITOTENV.2017.02.224

INFARMED, 2018. Meio ambulatório monitorização do consumo de medicamentos.

INFARMED, 2017. Estatística do medicamento e produtos saúde.

Jaria, G., Calisto, V., Gil, M.V., Otero, M., Esteves, V.I., 2015. Removal of fluoxetine from water by adsorbent materials produced from paper mill sludge. J. Colloid Interface Sci. 448, 32–40. https://doi.org/10.1016/J.JCIS.2015.02.002

Kadhim, Z.A., 2014. Evaluation of microalgae for secondary and tertiary wastewater treatment. Carleton University.

Kosmulski, M., 2009. Surface charging and points of zero charge. CRC Press.

Kumar, K.V., Porkodi, K., Rocha, F., 2008. Isotherms and thermodynamics by linear and non-linear regression analysis for the sorption of methylene blue onto activated carbon: Comparison of various error functions. J. Hazard. Mater. 151, 794–804. https://doi.org/10.1016/J.JHAZMAT.2007.06.056

Kumar, M.S., Kabra, A.N., Min, B., El-Dalatony, M.M., Xiong, J., Thajuddin, N., Lee, D.S., Jeon, B.-H., 2016. Insecticides induced biochemical changes in freshwater microalga Chlamydomonas mexicana. Environ. Sci. Pollut. Res. 23, 1091–1099.

https://doi.org/10.1007/s11356-015-4681-6

Kümmerer, K., 2004. Pharmaceuticals in the environment: sources, fate, effects and risks, Pharmaceuticals in the Environment. Springer Berlin Heidelberg, Berlin, Heidelberg. https://doi.org/10.1007/978-3-662-09259-0_1

Kümmerer, K., Hempel, M., 2010. Green and sustainable pharmacy. Springer.

Kwon, J.-W., Armbrust, K.L., 2006. Laboratory persistence and fate of fluoxetine in aquatic environments. Environ. Toxicol. Chem. 25, 2561. https://doi.org/10.1897/05-613R.1

Lagergren, S., 1898. About theory of so-called adsorption of soluble substances. K. Sven. Vetenskapsakademiens Handl. 24.

Lajeunesse, A., Smyth, S.A., Barclay, K., Sauvé, S., Gagnon, C., 2012. Distribution of antidepressant residues in wastewater and biosolids following different treatment processes by municipal wastewater treatment plants in Canada. Water Res. 46, 5600–5612. https://doi.org/10.1016/j.watres.2012.07.042

Langmuir, I., 1918. The adsorption of gases on plane surfaces of glass, mica and platinum. J. Am. Chem. Soc. 40, 1361–1403. https://doi.org/10.1021/ja02242a004

Largitte, L., Pasquier, R., 2016. A review of the kinetics adsorption models and their application to the adsorption of lead by an activated carbon. Chem. Eng. Res. Des. 109, 495–504. https://doi.org/10.1016/j.cherd.2016.02.006

Low, M.J.D., 1960. Kinetics of Chemisorption of Gases on Solids. Chem. Rev. 60, 267–312. https://doi.org/10.1021/cr60205a003

Lu, L., Yang, G., Zhu, B., Pan, K., 2017. A comparative study on three quantitating methods of microalgal biomass, Indian Journal of Geo Marine Sciences.

Martcheva, M., 2015. Introduction to mathematical epidemiology.

Merck KGaA, 2019. Fluoxetine hydrochloride [WWW Document]. URL http://www.merckmillipore.com/PT/en/product/Fluoxetine-Hydrochloride-CAS-56296-78-7-Calbiochem,EMD_BIO-343290?bd=1#documentation (accessed 3.26.19).

Millsap, R.E., Maydeu-Olivares, A., 2009. The Sage handbook of quantitative methods in psychology. Sage.

Mishra, Neha, Mishra, Neetu, 2017. Utilization of microalgae for integrated biomass production and phycoremediation of wastewater.

Montgomery, D.C., Runger, G.C., 2011. Applied statistics and probability for engineers. Wiley.

OECD, 2011. Test No. 201: Alga, Growth Inhibition Test, OECD Guidelines for the Testing of Chemicals, Section 2: Effects on Biotic Systems. OECD Publishing. https://doi.org/10.1787/9789264069923-en

Pereira, A.M.P.T.., Silva, L.J.G.., Lino, C.M.., Meisel, L.M.., Pena, A., 2015. Assessing environmental risk of pharmaceuticals in Portugal: An approach for the selection of the Portuguese monitoring stations in line with Directive 2013/39/EU. Chemosphere 144, 2507–2515. https://doi.org/10.1016/j.chemosphere.2015.10.100

Pereira, A.M.P.T., Silva, L.J.. G., Meisel, L.M., Lino, C.M., Pena, A., 2014. Environmental impact of pharmaceuticals from Portuguese wastewaters: geographical and seasonal occurrence,

removal and risk assessment. Environ. Res. 136, 108–119. https://doi.org/10.1016/j.envres.2014.09.041

Petrović, M., Perez, S., Barceló, D., 2013. Analysis, removal, effects and risk of pharmaceuticals in the water cycle : occurrence and transformation in the environment. Elsevier Science.

PubChem, 2019. Chlorofyll a compound [WWW Document]. Natl. Cent. Biotechnol. Inf. URL https://pubchem.ncbi.nlm.nih.gov/compound/Chlorophyll-a

Radjenovic, J., Petrovic, M., Barceló, D., 2006. Analysis of pharmaceuticals in wastewater and removal using a membrane bioreactor. https://doi.org/10.1007/s00216-006-0883-6

Rangabhashiyam, S., Balasubramanian, P., 2019. Characteristics, performances, equilibrium and kinetic modeling aspects of heavy metal removal using algae. Bioresour. Technol. Reports 5, 261–279. https://doi.org/10.1016/J.BITEB.2018.07.009

Ravishankar, G.A., Ramakrishna, A., 2016. Serotonin and melatonin: their functional role in plants, food, phytomedicine, and human health.

Redlich, O., Peterson, D.L., 1959. A Useful Adsorption Isotherm. J. Phys. Chem. 63, 1024–1024. https://doi.org/10.1021/j150576a611

Rivera-Utrilla, J., Bautista-Toledo, I., Ferro-García, M.A., Moreno-Castilla, C., 2001. Activated carbon surface modifications by adsorption of bacteria and their effect on aqueous lead adsorption. J. Chem. Technol. Biotechnol. 76, 1209–1215. https://doi.org/10.1002/jctb.506

Safi, C., Zebib, B., Merah, O., Pontalier, P.-Y., Vaca-Garcia, C., 2019. Morphology, composition, production, processing and applications of Chlorella vulgaris: A review. https://doi.org/10.1016/j.rser.2014.04.007ï

Santa Cruz Biotechnology, 2019. Fuoxetine hydrochloride [WWW Document]. URL www.scbt.com/scbt/product/fluoxetine-hydrochloride-56296-78-7 (accessed 3.26.19).

Schneider, J.D., 2018. Effects on the sorption of fluoxetine and sulfamethoxazole by three powdered activated carbons. Utah State University.

Sebastine, I.M., Wakeman, R.J., 2003. Consumption and Environmental Hazards of Pharmaceutical Substances in the UK. Process Saf. Environ. Prot. 81, 229–235. https://doi.org/10.1205/095758203322299743

Serra, A., 2015. Process and product control in an industrial scale microalgae production plant. Instituto Superior Técnico de Lisboa.

Silva, A., Stawiński, W., Romacho, J., Santos, L.H.M.L.M., Figueiredo, S.A., Freitas, O.M., Delerue-Matos, C., 2019. Adsorption of Fluoxetine and Venlafaxine onto the Marine Seaweed Bifurcaria bifurcata. Environ. Eng. Sci. 36, 573–582. https://doi.org/10.1089/ees.2018.0332

Sips, R., 1948. On the Structure of a Catalyst Surface. J. Chem. Phys. 16, 490–495. https://doi.org/10.1063/1.1746922

Sonune, A., Ghate, R., 2004. Developments in wastewater treatment methods. Desalination 167, 55–63. https://doi.org/10.1016/J.DESAL.2004.06.113

Spiess, A.-N., Neumeyer, N., 2010. An evaluation of R2 as an inadequate measure for nonlinear models in pharmacological and biochemical research: a Monte Carlo approach.

https://doi.org/10.1186/1471-2210-10-6

Tam, N.F.., Chong, A.M.., Wong, Y.S., 2002. Removal of tributyltin (TBT) by live and dead microalgal cells. Mar. Pollut. Bull. 45, 362–371. https://doi.org/10.1016/S0025-326X(02)00184-4

Tóth, J., 1971. State Equation of the Solid-gas Interface Layers. Acta Chim. Hung. 69, 311–328.

U.S. Environmental Protection Agency, 2002. Methods for Measuring the Acute Toxicity of Effluents and Receiving Waters to Freshwater and Marine Organisms EPA-821-R-02-012.

Udoh, A., Akbulut, A., Yildiz, K., Guler, D., 2012. Fourier transform infrared (FTIR) spectroscopy for identification of Chlorella vulgaris Beijerinck 1890 and Scenedesmus obliquus (Turpin) Kützing 1833. AFRICAN J. Biotechnol. 11. https://doi.org/10.5897/AJB11.1863

Weber;, W.J., Morris, J.C., 1962. Advances in water pollution research: removal of biologically resistant pollutants from wastewaters by adsorption. Adv. water Pollut. Res. Remov. Biol. Resist. Pollut. from wastewaters by Adsorpt. Proc. Int. Conf. Water Pollut. Symp. 231–266.

Wilt, H., 2018. Pharmaceutical removal: synergy between biological and chemical processes for wastewater treatment. Wageningen University. https://doi.org/10.18174/426133

Xie, Y., Li, H., Wang, X., Ng, I.-S., Lu, Y., Jing, K., 2014. Kinetic simulating of Cr(VI) removal by the waste Chlorella vulgaris biomass. J. Taiwan Inst. Chem. Eng. 45, 1773–1782. https://doi.org/10.1016/j.jtice.2014.02.016

Xiong, J.-Q., Kurade, M.B., Jeon, B.-H., 2018. Can microalgae remove pharmaceutical contaminants from water? Trends Biotechnol. 36, 30–44. https://doi.org/10.1016/J.TIBTECH.2017.09.003

Yamagishi, T., Yamaguchi, H., Suzuki, S., Horie, Y., Tatarazako, N., 2017. Cell reproductive patterns in the green alga Pseudokirchneriella subcapitata (=Selenastrum capricornutum) and their variations under exposure to the typical toxicants potassium dichromate and 3,5-DCP. PLoS One 12, e0171259. https://doi.org/10.1371/journal.pone.0171259

Yildiz, B.S., 2012. Water and wastewater treatment: biological processes. Metrop. Sustain. 406–428. https://doi.org/10.1533/9780857096463.3.406

Zhao, Q., Chen, A.-N., Hu, S.-X., Liu, Q., Chen, M., Liu, L., Shao, C.-L., Tang, X.-X., Wang, C.-Y., 2018. Microalgal microscale model for microalgal growth inhibition evaluation of marine natural products. Nat. Res. J. https://doi.org/10.1038/s41598-018-28980-z

Appendix A

A.1 Calibration curve – Biomass concentration and fluorescence

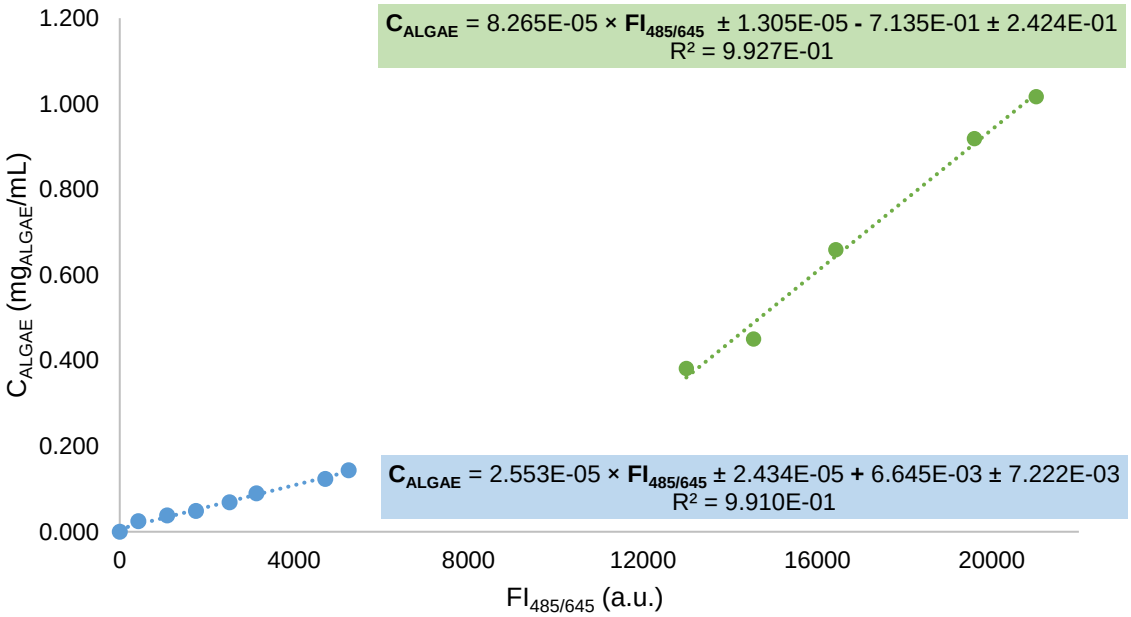

Figure A. 1. Calibration curve - biomass concentration and fluorescence for low and high concentration.

Appendix B

B.1 Chromatogram of standard solution of 2 mg/L fluoxetine

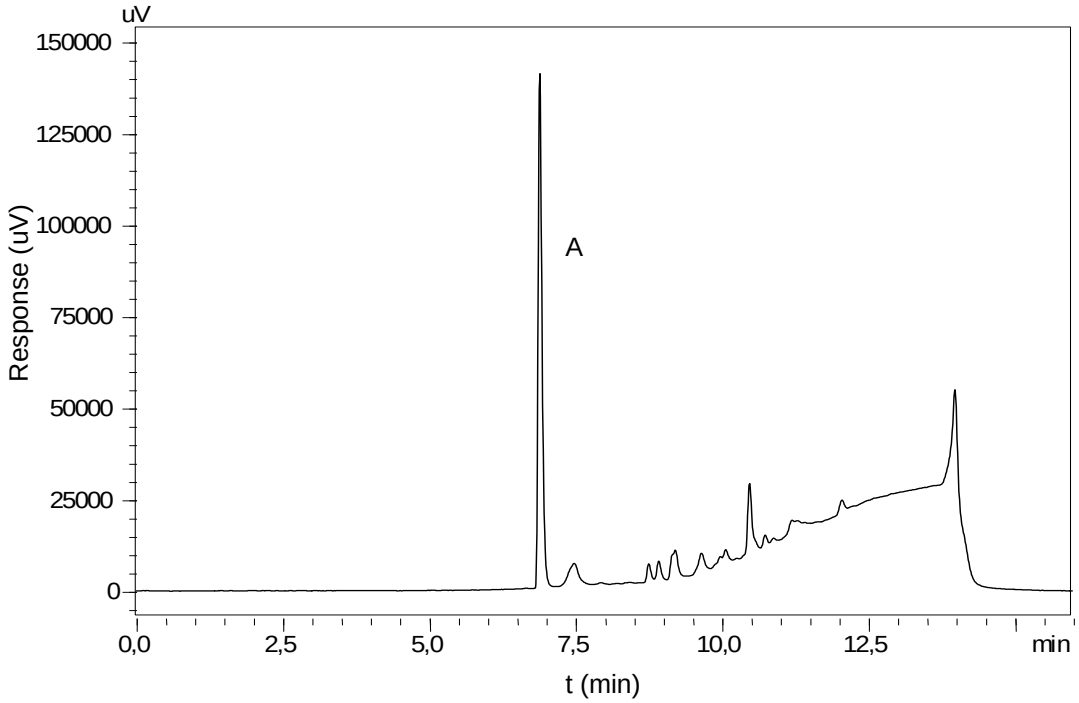

Figure B. 1. Chromatogram of standard solution of 2 mg/L fluoxetine (A – fluxetine peak).

B.2 Calibration curve –Peak Area and fluoxetine concentration

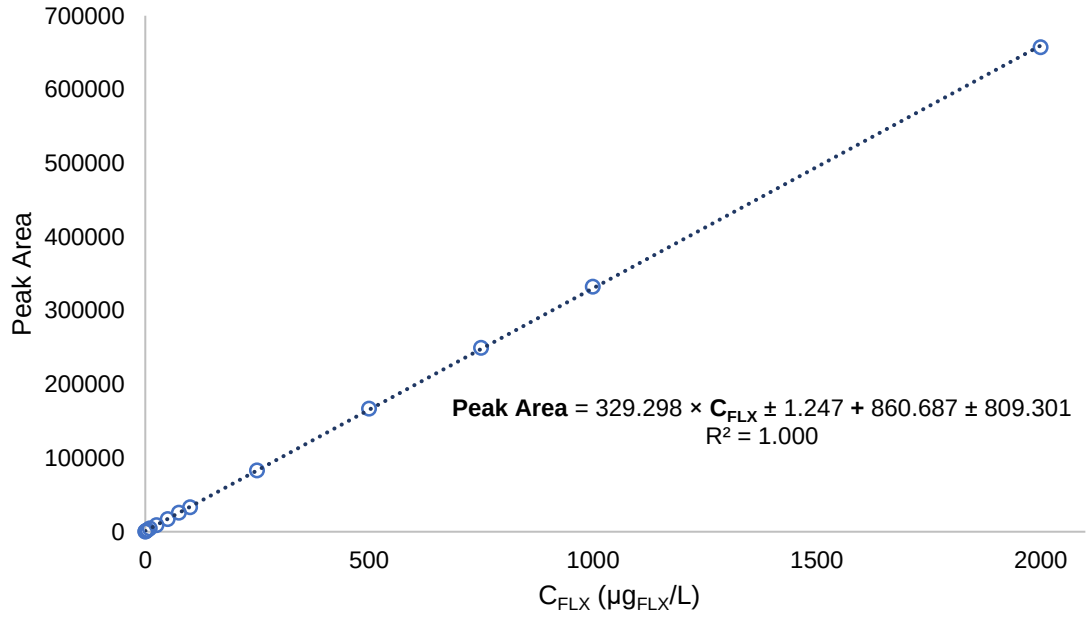

Figure B. 2. Calibration curve - peak area and fluoxetine concentration.